NON-GIMBALED ANTENNA POINTING-
SUMMARY OF RESULTS AND ANALYSIS

Stephen Horan

NMSU-ECE-98-001 March 23, 1998

Non-Gimbaled Antenna Pointing - Summary of Results and Analysis

Prepared by

Stephen Horan
Manuel J. Lujan Space Tele-Engineering Program
Klipsch School of Electrical and Computer Engineering
New Mexico State University
Box 30001, MSC 3-O
Las Cruces, NM 88003

NMSU Technical Report NMSU-ECE-98-001

Prepared under NASA Research Grant NAG 5-1491

March 23, 1998

Table of Contents

ACRONYM LIST

AOS	Acquisition of Signal
E_b/N_0	Energy per bit to noise density ratio
BER	Bit Error Rate
EIRP	Effective Isotropic Radiated Power
EUVE	Extreme Ultra Violet Explorer
JPL	Jet Propulsion Laboratory
K	TDRS Service-Specific Constant
LEO	Low Earth Orbit
LOS	Loss of Signal
NASA	National Aeronautics and Space Administration
SMA	S-band Multiple Access
SN	Space Network
SNUG	Space Network User's Guide
STK	Satellite Tool Kit
TDRS	Tracking and Data Relay Satellite
TDRSS	Tracking and Data Relay Satellite System
TOPEX	Ocean Topography Explorer
WSC	White Sands Complex
ZOE	Zone of Exclusion

SECTION 1 - BACKGROUND

1.1 MOTIVATION

There is considerable interest at this time in developing small satellites for quick-turnaround missions to investigate near-earth phenomena from space; see, for example [1]. One problem to be solved in mission planning is the means of communication between the control infrastructure in the ground segment and the satellite in the space segment. A nominal small-satellite mission design often includes an omni-directional or similar wide-pattern antenna on the satellite and a dedicated ground station for telemetry, tracking, and command support. These terminals typically provide up to 15 minutes of coverage during an orbit that is within the visibility of the ground station; however, not all orbits will pass over the ground station so that coverage gaps will exist in the data flow. To overcome this general limitation on data transmission for low-earth orbiting satellites, the Space Network (SN), operated by the National Aeronautics and Space Administration, (NASA) has been designed to transmit data to and from user satellites through the Tracking and Data Relay Satellites (TDRS) in geostationary orbit and interfacing to the White Sands Complex (WSC) in New Mexico for the data's ground entry point. The advantage of the SN over a fixed ground station is that all low-earth-satellite orbits will be within the visibility area of at least one TDRS within the SN for a large part of the orbit and the potential exists to establish a communications link if the user satellite can point an antenna in the direction of any one of the relay satellites. Within NASA, there is considerable interest in seeing that small satellite developers are aware of the advantages to the SN and that designs to include the SN are part of the satellite design[2]. Small satellite users have not often considered using the SN because of

1. The 26-dB link penalty differential between direct broadcast to a ground station and transmission through a TDRS to the ground
2. The class of satellite is too small to support high-gain antennas and associated attitude control and drive electronics
3. The class of satellites is severely weight and power limited
4. There are perceived problems in scheduling communications for this class of user on the SN

This report addresses the potential for SN access using non-gimbaled, i.e. fixed-pointed, antennas in the design of the small satellite using modest transmission power to achieve the necessary space-to-ground transmissions. The advantage of using the SN is in the reduction of mission costs arising from using the SN infrastructure instead of a dedicated, proprietary ground station using a similar type of communications package. From the simulations and analysis presented, we will show that a modest satellite configuration can be used with the space network to achieve the data transmission goals of a number of users and thereby rival the performance achieved with proprietary ground stations. In this study, we will concentrate on the return data link (from the user satellite through a TDRS to the ground data entry point). The forward command link (from the ground data entry point through a TDRS to the user satellite) will usually be a lower data rate service and the data volume will also be considerably lower than the return link's requirements. Therefore, we assume that if the return link requirements are satisfied, then the forward link requirements can also be satisfied.

The constellation of six TDRS satellites are spread around the earth's equator as illustrated in Figure 1. Also shown is the location of the control terminal at the WSC. The longitudinal locations of each satellite are given in Table 1.

For simulation purposes in the studies reported here, only the nominal TDRS East, West, and Zone of Exclusion (ZOE) satellites will be used. All of the remaining satellites will be considered to be constellation on-orbit spares and not available for services. For the actual experiments used in these studies, only TDRS East and West were used for data services. Each TDRS can support K-band and S-band single-access communications and S-band multiple access communications [3]. The choice of the TDRS to be used on a given data service depends on the relative satellite positions, the availability of communications links, and the requested service duration. The data link between the SN and the ground communications networks is run through the WSC facility which interfaces with the user satellite's control center utilizing NASA's communications links. Presently, the S-band multiple access service has the greatest probability of availability to the small satellite user so it is used in the data throughput analysis. The SMA service uses code division multiplexing with each user having a return carrier frequency of 2287.5 MHz. This investigation looks at two possible SN access modes: a single TDRS is available to support access and the possibility of using the full constellation of three operational TDRS spacecraft forming the full SN constellation.

The data and analysis in this report are based on previously-issued reports [4] - [11] with some additional computations to round out the presentations made there.

In the next section, we look at the communications access times for fixed ground stations and follow that with a description of the simulation methodology and the baseline configuration for the small satellite communications system. Section 2 describes the results of the simulations conducted for nadir-pointed satellites and inertially-controlled satellites. Section 3 describes the tests conducted with the TOPEX and EUVE satellites through the SN. Section 4 presents the computations made to determine the data throughput available based upon fixed EIRP assumptions and EIRP requirements based on data throughput needs. Section 5 describes recommendations based on the tests and simulations conducted here.

1.2 DIRECT BROADCAST TO GROUND STATIONS

We take as our starting point in this study, the typical small satellite communications configuration where data is directly broadcast to one or more fixed ground stations. In particular, we wish to learn what transmission duration can be provided to a Low Earth Orbit (LEO) satellite communicating with such a fixed ground station. The answer to this question will depend upon the LEO satellite's altitude, orbital inclination angle, and the latitude of the ground station. To see an example of this configuration, we consider a LEO satellite with an altitude of 705 km and a sun-synchronous orbital inclination. Furthermore, we consider ground stations in Alaska, New Mexico, and Guam to represent "typical" ground station locations. A series of orbital simulations were performed with Satellite Tool Kit (STK) [12] and a typical ground track is shown in Figure 2. The average available

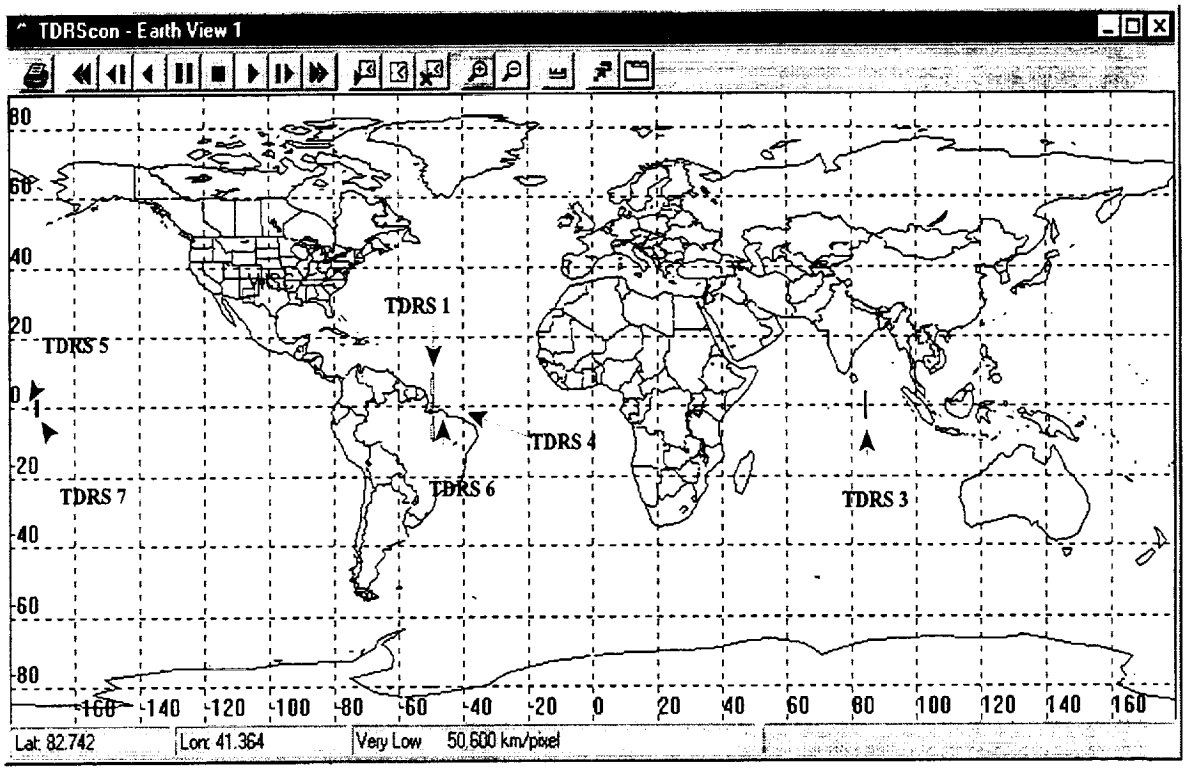

Figure 1 - Location of the TDRS constellation of satellites within the SN.

Table 1. TDRS Constellation Description			
TDRS	**Catalog Number**	**Longitude**	**Other**
1	13969	49° W	TDRS Spare
3	19548	275° W	TDRS ZOE
4	19883	41° W	TDRS East
5	21639	174° W	TDRS West
6	22314	47° W	
7	23613	171° W	

access times per satellite pass and number of passes per day over the ground station are given in Table 2. Typically, a LEO satellite will have 7 to 7½ minutes of contact when the LEO satellite is at least 10 degrees above the local horizon.

If the LEO satellite's orbital inclination were closer to 0°, then the access durations will be more variable at each ground station. For example, as listed in Table 3, a LEO satellite with a 28.5-degree

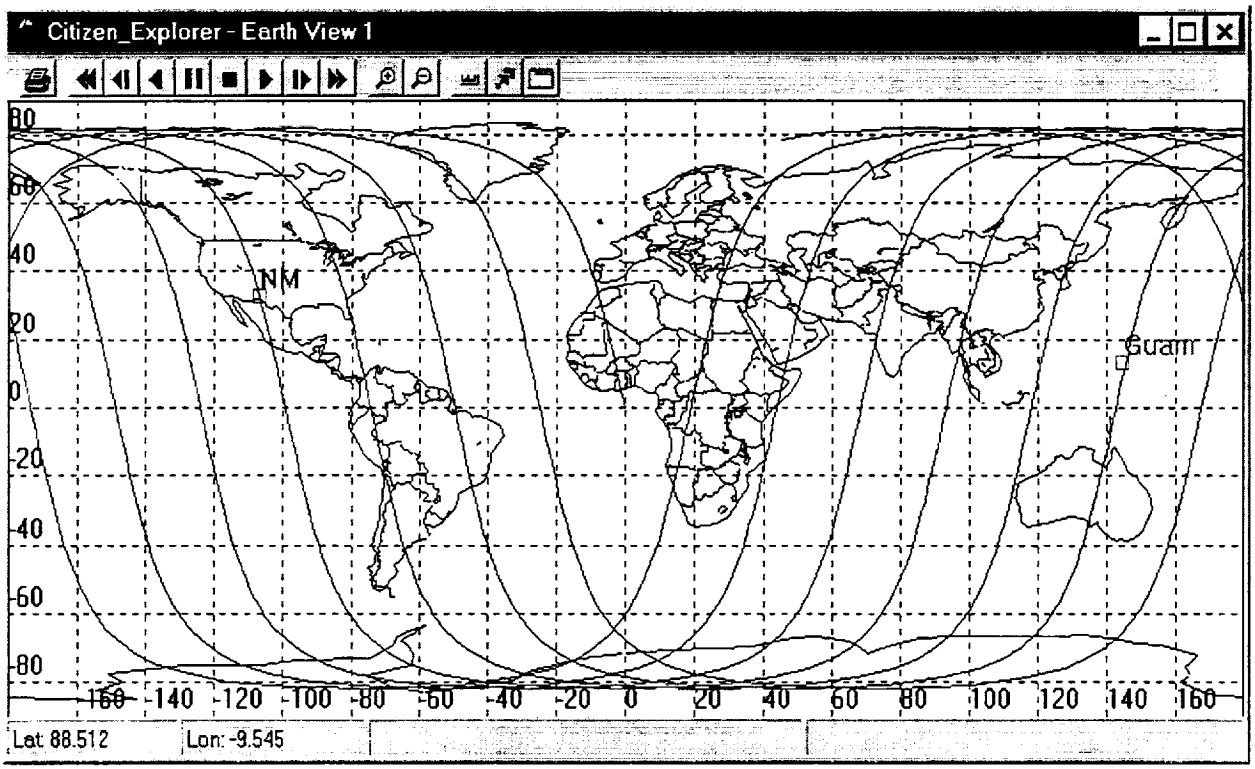

Figure 2 - Sample ground tracks for a sun-synchronous LEO satellite with an altitude of 705 km.

Table 2. Simulated Sun-Synchronous LEO Satellite Ground Station Access		
Ground Station	**Average Access Time (minutes)**	**Average Daily Passes**
Alaska	7.08	9.35
New Mexico	7.48	3.52
Guam	7.69	2.90

inclination orbit will not have a contact at the Alaska ground station and will have shorter access times at the New Mexico and Guam ground stations. Notice, however, that the number of contacts per day increases with the lower inclination orbit. The exact pattern for any given LEO satellite will be a function of the satellite's orbital elements and the ground station location.

A goal of this study is to determine if the SN can improve this situation by providing enough contacts of sufficient duration to support a significant data transport volume. If the access durations

Table 3. Simulated 28.5° Inclination LEO Satellite Ground Station Access		
Ground Station	**Average Access Time (minutes)**	**Average Daily Passes**
Alaska	not available	
New Mexico	5.13	4.13
Guam	4.90	5.23

are long enough, the next step is to investigate the communications system requirements to provide a closed link at an acceptable Bit Error Rate (BER) performance. The ultimate goal is to provide a competitive daily data throughput volume at a competitive grade of service even though there is a significant link penalty to using the SN.

1.3 CLASS OF USERS TO BE SUPPORTED

The non-gimbaled antenna pointing concept was developed to service the needs of the low data rate users in the small satellite community. It is expected that the large, high-data-rate satellites would be designed with the gimbaled antennas and high-power communications systems required to support the necessary data throughput for the satellite's mission. The low-data-rate small satellite users were expected to be candidates for the fixed-antenna technique because the link penalty caused by transmitting to a geostationary satellite will be partially overcome in the link budget if the data rate is relatively low. In particular, we are concerned with addressing the needs of users whose average data volume for space-to-ground transmission is equivalent to a 10 kbps continuous link or less. This figure represents approximately 50% of the class of small satellite users [13].

For the conceptual design of a small satellite system, we make the following assumptions as the initial system baseline for the communications subsystem:

a. the communications subsystem is able to supply an output power of 10 Watts to the antenna system;
b. the antenna system can provide a gain of at least 5 dB over internal losses, pointing losses, polarization loses, etc.;
c. the satellite is nadir-pointing and aligned along the radial vector connecting the satellite with the center of the earth;
d. the antenna system is surface mounted pointing towards the local zenith and away from the center of the earth;
e. communications contact between the satellite and the SN can be initiated as the satellite sweeps past a TDRS position in its orbit as illustrated in Figure 3;
f. a SN S-Band Multiple-Access (SMA) service can be used for the communications link; this

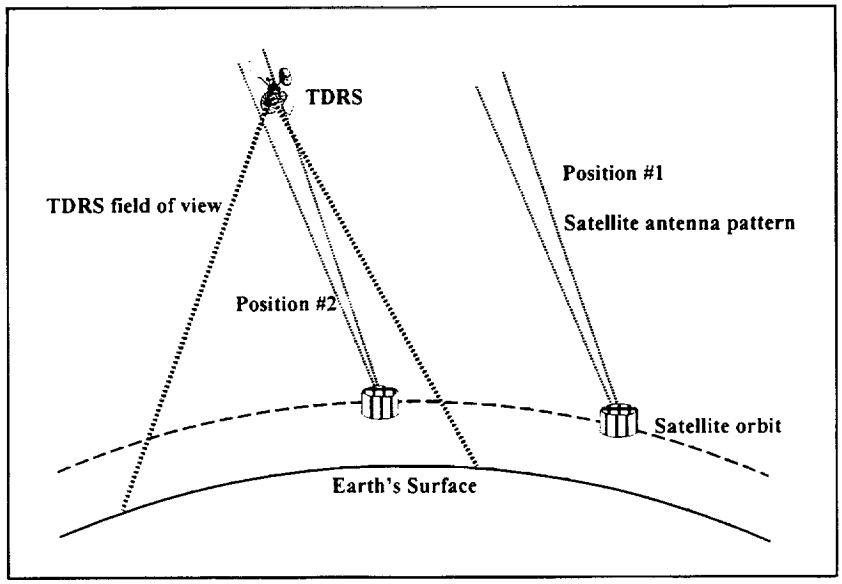

Figure 3 - TDRS-to-satellite access geometry. In position #1, no access between a TDRS and the user satellite is not possible while in position #2, access is possible.

implies that the TDRS antenna is capable of tracking the satellite using open-loop techniques.

Using these restrictions, we will determine if this minimal baseline system can accomplish the desired goal of data transport and grade of service.

1.4 ANALYSIS TECHNIQUE

The analysis of the orbital motions used in this study were performed using the software package Satellite Tool Kit. This package was run on PC running Windows 95. Both versions 3 and 4 of the product were run. Orbital elements for the TDRS satellites were taken from the Air Force Institute of Technology [14] and updated as needed for the simulations or analyzing the actual experiments.

1.5 VERIFICATION TECHNIQUE

The orbital analysis results were checked in two modes. First, the results were compared with similar simulations run using other packages, including both commercial orbital analysis packages and locally-developed analysis. Secondly, the orbital analysis was used to predict times for actual spacecraft and TDRS communications opportunities. In these cases, the predicted performances were found to match the actual satellite access profiles. From these checks, we believe that the results of the analysis are correct.

SECTION 2 - ORBITAL ACCESS SIMULATIONS

2.1 SIMULATION CONFIGURATION

To determine if using the space network can be an effective alternative to the fixed ground station model we first need to determine the access potential for a simple satellite communications system. The computer simulation package Satellite Tool Kit was used to predict the three-dimensional positions of all three TDRS and model user satellite. For the studies, a one-month time period was simulated. This period covers all of the contact variations in the orbits. For the simulations, the mean orbital elements for the TDRS positions were taken from [14] and the elements used for a sample set of simulations are listed in Table 4. Satellite Tool Kit propagates the orbital elements over the 30-day period for each satellite to account for the perturbations caused by the variations in the earth's gravitational field. For the simulations, an attitude control model for the model user satellite is required. This is entered as part of the simulation configuration along with initial orbital elements for the type of satellite simulation desired.

In Satellite Tool Kit, antennas on satellites were modeled as "sensor objects" in the simulation having an associated field of view for determining visibility and access. Each sensor object has a conical field of view with a half angle describing the width of the conic and a positioning direction defined relative to the satellite. For purposes of simulation, the half angle of the conical field of view was taken to be one-half of the antenna's Half Power Beam Width (HPBW) as illustrated in Figure 4. The simulated satellites were given antenna pointing based on the type of model being simulated and the antenna's field-of-view half-angle was varied according to which antenna HPBW was being simulated. For each TDRS, the SMA antenna was modeled, based on its steerable field-of-view, with a conical field of view of $\pm 13^\circ$ rather than the HPBW of the SMA array and an initial positioning direction towards the center of the earth. In the simulations, an access of a TDRS by a LEO satellite occurs when the field-of-view computation shows that both antenna systems are mutually visible as is illustrated in Figure 3. The simulation analysis recorded the start and stop time of each access period between the LEO satellite and each TDRS, the pointing angles, and the slant range between the satellites.

2.2 CASES STUDIED

There were two general classes of attitude control for the LEO satellite studied with the simulation analysis:

a. nadir-pointing satellites
b. inertially-stabilized satellites

In the first case, we assumed that the satellite is designed to point at the earth's surface and the communications antenna is mounted so that it points away from the earth along a radial vector.

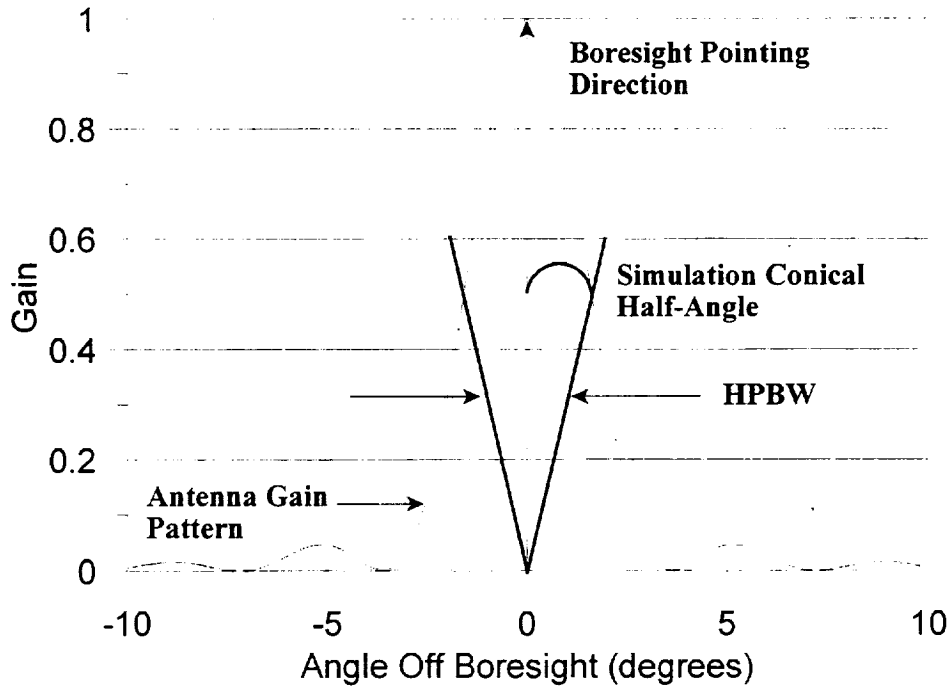

Figure 4 - Relationship between antenna HPBW, simulation conical half-angle, and boresight pointing direction.

Table 4. Typical Tracking and Data Relay Satellite Orbital Elements

element	TDRS East	TDRS West	TDRS-Z
eccentricity	0.0003746	0.00003342	0.000555
right ascension of the ascending node	86.2181°	93.3433°	70.5384°
argument of perigee	216.5846°	243.3013°	221.1338°
mean anomaly	324.2369°	186.8302°	184.2067°
mean motion (rev/day)	1.00266752	1.00272053	1.00270378
inclination angle	0.3747°	0.0373°	2.9472°
epoch (1997)	46.4517419	48.52874914	34.71312596

In this case, the satellite is simulated as having a fixed antenna pointing towards the satellite's local zenith position. The second case considers a satellite with inertial stability and the antenna is mounted pointing away from the earth. This type of satellite does not normally spin but may be moved to various orientations based on the mission needs.

2.2.1 Nadir-Pointing Satellite

A set of simulations between LEO user satellites and the TDRS constellation was run with a STK attitude control model set to correspond to a nadir-pointing, spin-stabilized satellite. In the various simulation runs, the user LEO satellite was given orbital elements corresponding to an altitude between 600 km and 1200 km. The orbital inclination angle for the set of simulations was varied from 0° through 100°. Two commonly-used orbital inclination angles from this set are reported here: 28.5° and sun-synchronous. The other orbital elements for the spin-stabilized satellite, Right Ascension of Ascending Node, Argument of Perigee, and Mean Anomaly, were set to 0° since we were not interested in predicting an exact position of a real satellite but determine general access characteristics.

The orbital inclination angle, i, for a sun-synchronous orbit is a function of the orbital altitude and is given by [15]

$$i = \cos^{-1}\left[\frac{0.9856^{o}/day}{(-\frac{3}{2})J_2\sqrt{\frac{\mu}{(R+h)^3}}\left[\frac{R}{(1-e^2)(R+h)}\right]^2}\right]$$

Here, R is the radius of the earth, h is the mean orbital height, J_2 is the second-order gravitational zonal harmonic coefficient, e is the orbital eccentricity (assumed to be 0), and μ is the product of the universal gravitational constant and the mass of the earth. Table 5 gives the sun-synchronous orbital inclination angle as a function of orbital altitude.

2.2.2 Inertially-Stabilized Satellite

Most inertially-stabilized satellites are large enough that fixed antenna pointing is not normally considered for space-to-space communications. It may be considered for space-to-ground communications as either a normal transmission more or as an emergency transmission mode. Questions have been submitted to the investigators as to whether the fixed antenna concept would still hold in this case, and if it does, is there a preferred location for such an antenna on the satellite structure? In trying to emulate the action of a nadir-pointing satellite with an inertially-stabilized satellite, the Extreme Ultra Violet Explorer (EUVE), was used as a test vehicle.

During the test passes, the expected access time was predicted to be approximately five minutes centered on the time when EUVE was closest to TDRS West. Because the EUVE antenna system has a significant gain and a correspondingly narrow antenna pattern, an accommodation was needed to make the test similar to that predicted to be found with a broad-beam antenna sweeping past the

Table 5. Sun-synchronous Orbital Inclination Angle as a Function Orbital Altitude	
Altitude (km)	**Inclination Angle (degrees)**
600	97.8
700	98.2
800	98.6
900	99.0
1000	99.5
1100	99.9
1200	100.4

TDRS location. To accomplish this, the EUVE control center pointed the spacecraft antenna to the TDRS position at the time of closest approach and fixed it there for the pass duration. This pointing was done prior to the start of the pass and active pointing during the pass was disabled by ground command. During the test passes, it was expected that, as EUVE moved along its orbit, it would sweep past the TDRS position and emulate the desired contact profile. The results of these test contacts were that the contact times greatly exceeded the predicted value of five minutes. To allow for timing uncertainties and to allow for tracking of the receiver acquisition process, data were collected for a period of 30 minutes centered around the expected contact mid-point. Instead of a gradual acquisition and loss process at the start and end of the data acquisition interval during each pass, the ground station receivers immediately locked onto the EUVE communications signal relayed through TDRS at the scheduled start of the communications service time and stayed locked until the scheduled end of the service time. Therefore, instead of a five-minute pass, we recorded thirty-minute passes during each contact period. In subsequent discussions during the test debriefing, the reason for the unexpectedly long contact results became clear. The initial conceptual model for the test assumed that the communications antenna mounted on the EUVE spacecraft would act in a sweeping motion with respect to the TDRS SMA antenna since the EUVE antenna did not employ active tracking during the contact time. However, this model neglects the effects of having an inertially-stabilized attitude control system in EUVE. An inertially-stabilized attitude control system tries to maintain a constant pointing of the spacecraft with respect to an inertial coordinate system. While TDRS is still in earth orbit, its orbital altitude of 42,164 km with respect to the center of the earth and in excess of 35,000 km from EUVE, effectively places it at a distance of infinity with respect to EUVE and nearly motionless in an inertial coordinate system as seen from EUVE. Therefore, EUVE's inertial attitude control system maintains nearly-constant antenna pointing during a whole TDRS visibility period even though active antenna tracking has been disabled. With this type of spacecraft, the sweeping motion of a spinning satellite cannot be replicated without actively pointing the antenna during the pass. This also implies that active tracking during the pass may not be necessary to maintain communications contact between an orbiting spacecraft and TDRS.

2.3 PREDICTED ACCESS RESULTS

In this section we investigate the simulated access results for both attitude control models in the user spacecraft. We look at both single-TDRS coverage and whole-constellation coverage. We also investigate a variety of antenna HPBW in the simulations.

2.3.1 Nadir-Pointing Satellite

Using the simulations with the orbital altitude set between 600 and 1200 km, we investigated when there is a possibility for SN coverage under the constraint that a spin-stabilized, nadir-pointing satellite has no active positioning mechanism for the antenna. Rather, the satellite relies on its communications antenna sweeping past each of the TDRS locations within the SN to provide the contact opportunity. For the simulation parameters mentioned above, it was found that there was no time interval when more than one TDRS satellite location was simultaneously visible from the spin-stabilized satellite. This is in contrast to the normal gimbaled antenna design, there are times when a LEO satellite can be accessed by one of the two TDRS visible to it. It was also found that each of the three TDRS locations had similar results when averaged over the 30-day simulation period so only the results for TDRS-West, at -174° longitude, will be given here when discussing the results for a single TDRS. Figure 5 illustrates a 24-hour segment of the simulations using a 28.5° orbital inclination angle, a 600-km orbital altitude, and a 20° half-angle for the spin-stabilized satellite's antenna field-of-view. Highlighted positions within the circles centered on each TDRS position show the opportunities along the spin-stabilized satellite's ground track when the satellite can access each TDRS. If the ground tracks were shown for the full 30-day simulation period on a single plot, then the entirety of the circles would be filled by these highlighted regions along the nadir-pointed, spin-stabilized satellite's ground track.

From the simulations, we find that the orbital inclination angle and the antenna field of view of the spin-stabilized satellite control the contact durations and the number of contacts per day between that satellite and each TDRS. For the orbital altitudes considered here, the altitude does not affect the results to the same extent that the other parameters do. If the nadir-pointed, spin-stabilized satellite had an orbital inclination angle of 0°, then the simulations show that there would be a contact with each TDRS as the satellite swept under the TDRS subsatellite points and each contact would have a duration as determined by the antenna HPBW. As the orbital inclination angle grows, the simulation results show that the total number of contacts per day drops and not every orbit always receives a contact possibility. In the inclined-orbit cases, a maximal-length contact, limited only by the antenna HPBW, occurs for those orbits where either the orbital ascending node or descending node lies near the TDRS subsatellite point. Other orbits have contacts of shorter duration with polar orbits having the fewest contacts and shortest average contact duration. Figures 6 through 9 summarize the simulation results for the number of contacts and contact duration as averaged over the 30-day simulation periods. Each figure shows the results over the 600 through 1200-km orbital altitude range considered. Each figure is for a single orbital inclination angle and antenna field of view combination. The plots illustrate the average number of daily contacts through both a single TDRS

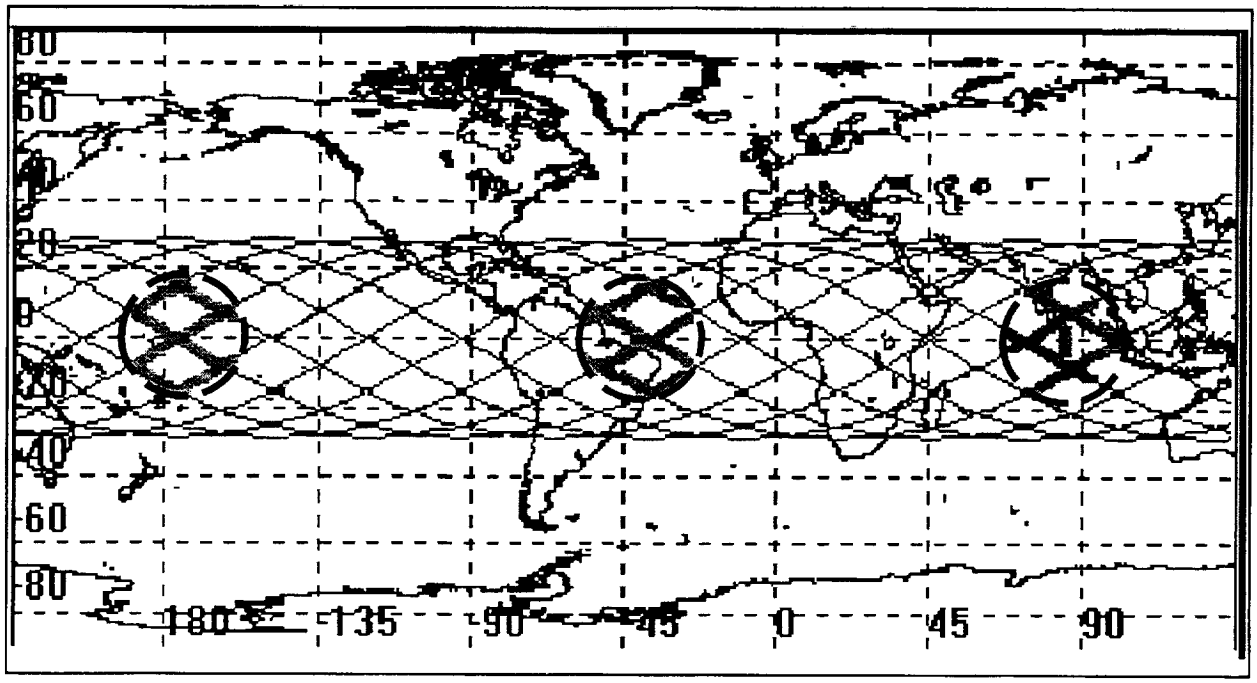

Figure 5 - Simulated 24-hour ground track for spinning-satellite contact with the Space Network. Highlighted areas within the circles along the ground track near the TDRS positions at -174°, -41°, and +85° longitude show times when contact is possible.

and the three-TDRS constellation, the average contact duration with a single TDRS, and the total average daily contact time through both a single TDRS and the constellation. Figure 6 illustrates the results for the case of a 28.5° orbital inclination and an antenna field of view of ±20°. Here, we find that the typical orbit will provide five contacts per day, each having an average duration of eight minutes yielding a total daily contact time of 40 minutes. The entire SN constellation would provide approximately 15 contacts per day at eight minutes per contact giving a total contact time of 120 minutes. Figure 7 illustrates the results for a ±45° antenna field of view at a 28.5° orbital inclination angle, Figure 8 uses a ±20° antenna field of view and a sun-synchronous orbital inclination angle, and Figure 9 uses a ±45° antenna field of view and a sun-synchronous orbital inclination angle. The contact information for each individual TDRS is similar to that of a low-earth orbit satellite accessing a fixed ground station. For example, using the same simulation software, we find that a satellite in a 900-km-altitude orbit communicating with a fixed ground station at 32.5° N would typically have 6.7 contacts per day with an average duration of 14.6 minutes for a total contact time of 98 minutes when the orbital inclination angle is 28.5°. When the orbit is sun synchronous, the same satellite and ground station configuration would have 5.5 contacts per day at 13 minutes per contact for a total contact time of 71.5 minutes. In this simulation study, we find that the SN constellation acts like a network of three fixed-location ground stations spread around the surface of the earth.

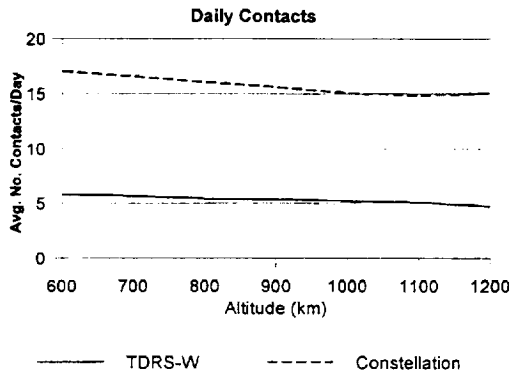

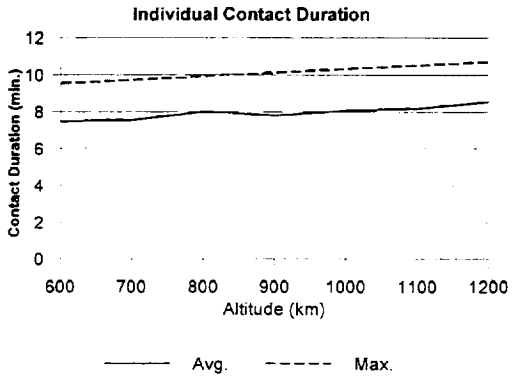

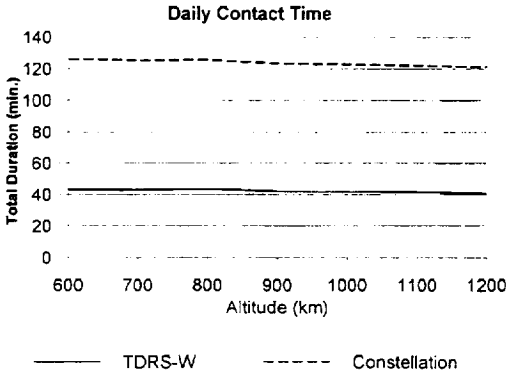

Figure 6 - Simulated number of contacts per day, single-TDRS contact duration, and total daily contact time for a 28° orbital inclination and ±20° field of view.

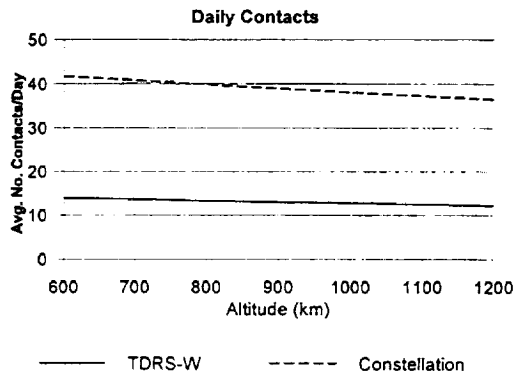

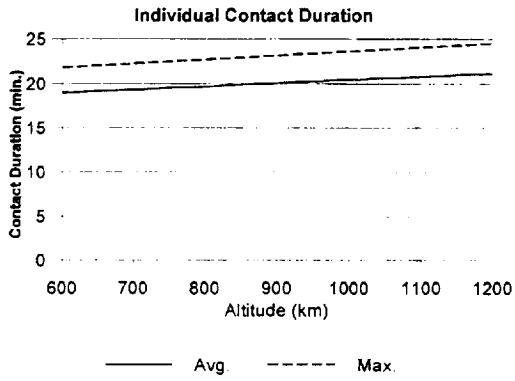

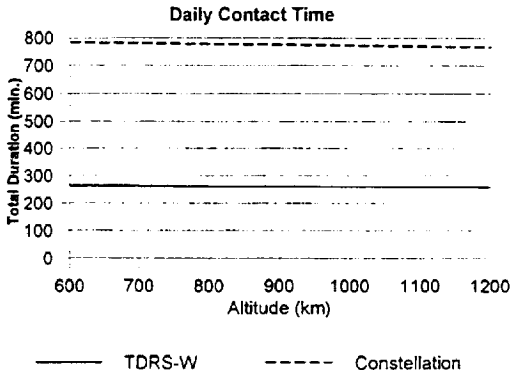

Figure 7 - Simulated number of contacts per day, single-TDRS contact duration, and total daily contact time for a 28° orbital inclination and ±45° field of view.

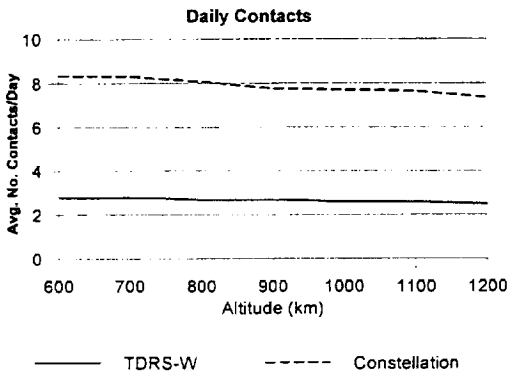

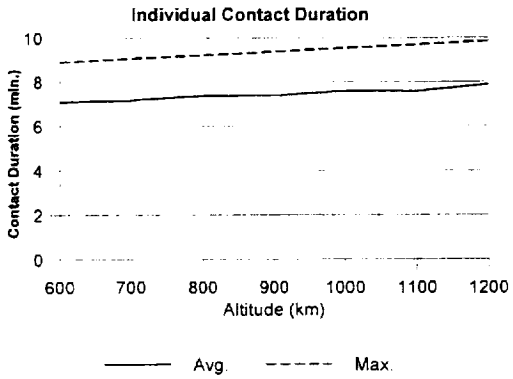

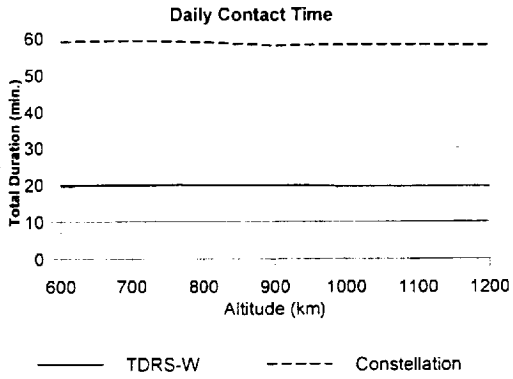

Figure 8 - Simulated number of contacts per day, single-TDRS contact duration, and total daily contact time for a sun-synchronous orbital inclination and ±20° field of view.

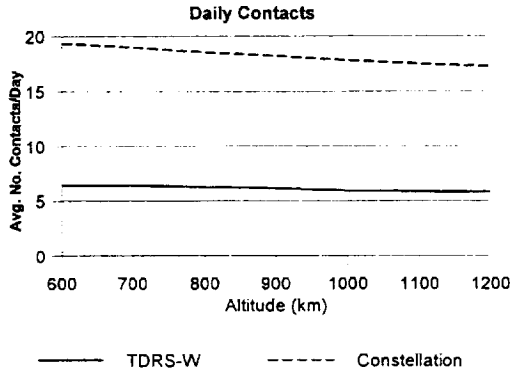

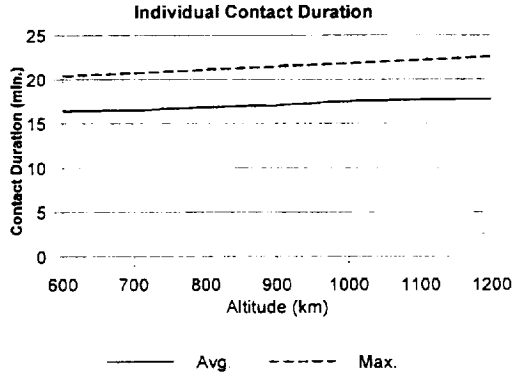

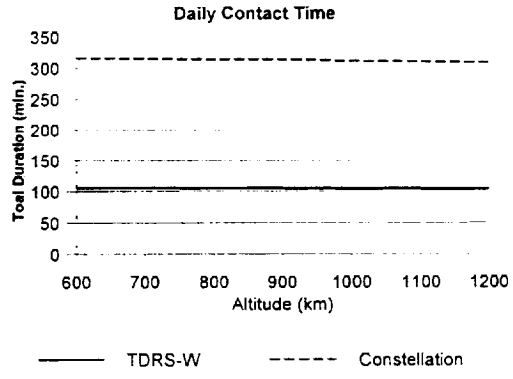

Figure 9 - Simulated number of contacts per day, single-TDRS contact duration, and total daily contact time for a sun-synchronous orbital inclination and ±45° field of view.

From the simulation studies, we can conclude that small orbital inclination angles or large antenna HPBW angles are needed to have large numbers of contact minutes per orbit and a large number of orbits per day on which a contact occurs. The penalty for having a fixed antenna or narrow HPBW angle is seen in the results illustrated in Figures 6 through 9 because some orbits have no contact time. However, this is similar to transmitting data to a single, fixed ground station where the contacts are clustered in two groups occurring twice each day.

The HPBW of the fixed antenna restricts total access since orbits can have times where no SN access is possible due to the angle between the simulated spin-stabilized satellite position and the relay satellites exceeding the HPBW angle. The short contact times and few number of contacts for a narrow antenna field of view is least at lower inclination angles and is worst at 90-degree inclination angles. For inclined orbits, the mitigation for the low total contact duration per day is to increase the antenna HPBW. For the ±45° field-of-view case, there are many instances where, on a given orbit, only one of the three TDRS satellites is visible while on the next orbit, a different TDRS is visible. Therefore, for the wide antenna HPBW case, there are relatively few orbits when at least one of the TDRS cannot be scheduled for short periods based on a visibility restriction.

The visibility needs to be balanced with the data rate support available with the different antenna gains. An antenna with a narrow HPBW will have a higher antenna gain than an antenna with a wider HPBW. The former antenna will be able to support a higher data rate with the same data quality. Therefore, the overall data throughput will be a function of both the contact duration and the data rate. In Section 4, we look at the throughput that is available based on both the access time and the data rate that can be supported.

2.3.2 Inertially-Stabilized Satellite

In order to better understand the actual test results and validate the hypothesis for the interaction between attitude control and antenna pointing, a series of simulations were performed. The orbital elements given in Table 6 were used to generate the TDRS and EUVE positions corresponding to the time of the actual satellite passes. The simulation used an inertial attitude control model for the EUVE spacecraft. The simulated TDRS was modeled as having a conical field of view of ±13° corresponding to the actual TDRS SMA antenna system pointing range. A conical field of view of ±6.2° was found to be the minimum necessary on the simulated LEO satellite to have contact with the simulated TDRS during whole time the TDRS was in view of the LEO satellite. A narrower field of view in the LEO satellite reduced the simulated contact time while a wider field of view did not increase the simulated contact time. By way of comparison, the actual EUVE antenna has a HPBW of approximately 7° which corresponds to a field of view that is one half that found necessary to maintain contact over the simulated duration. However, there is significantly more than 3 dB of link margin so the antenna actually performed more like the simulated antenna than the HPBW would indicate. In the simulations, the field of view is considered to be an absolute constraint for determining the start and stop of the contact. For real systems, the beamwidth allowed by the link margin is the relevant beam width to be used for determining the contact times. This will typically be more

Table 6. NORAD Two-Line Elements	
Satellite	**Mean Orbital Elements**
EUVE	1 21987U 92031A 96133.75979634 .00000715 00000-0 23180-4 0 5418 2 21987 28.4307 61.1763 0008917 26.4215 333.6854 15.19769324218282
TDRS 4 West	1 21639U 91054B 96134.58492492 .00000067 00000-0 00000+0 0 326 2 21639 0.0894 72.6418 0004855 340.4259 214.7824 1.00274365111549

Table 7. EUVE-to-TDRS Pass Log					
		Simulated (UT)		**Predicted (UT)**	
Day	**Pass**	**Start of Pass**	**End of Pass**	**AOS**	**LOS**
134	1	11:54:17	12:52:07	11:58:00	12:48:00
	2	13:34:46	14:33:04	13:39:00	14:29:00
	3	15:15:37	16:14:50	15:20:00	16:11:00
135	1	11:33:15	12:31:07	11:37:00	12:27:00
	2	13:13:44	14:12:08	13:18:00	14:08:00
	3	14:54:40	15:53:58	14:59:00	15:50:00

than the HPBW but the exact amount needs to be determined by the system designer based on the available link performance margin.

To compare the validity of the simulations with the actual test measurements, we give the times for the contacts over the period of the actual tests based on the simulations in Table 7. In this table, the contact times, as predicted by NASA prior to the tests, are also listed to show that they compare quite well. Ground tracks for all six of the simulated EUVE passes (light and heavy sinusoidal lines) and TDRS West (dot at the equator at -174° longitude) are shown in Figure 10. The heavy-lined section of the ground track for EUVE indicates the portion of a pass when a contact through TDRS West would be possible. The Acquisition of Signal (AOS) and Loss of Signal (LOS) points along the simulated ground track are indicated. To produce the ground track, the user must enter the orbital element sets into the simulation program and adjust the simulated EUVE yaw, pitch, and roll attitude to give boresight antenna pointing to the TDRS West position at the time of closest approach. This simulates the configuration of the actual EUVE antenna pointing during the passes.

From these results, we can predict that the entire 58-minute pass should have been observable and not just the 30 minutes over which data was collected. For the actual test passes, all but one were observed to have actual measurements during the entirety of the scheduled test time. The one that did not was due to a ground hardware configuration problem. This implies that non-active pointing

(a) Pass #1 of Day 134

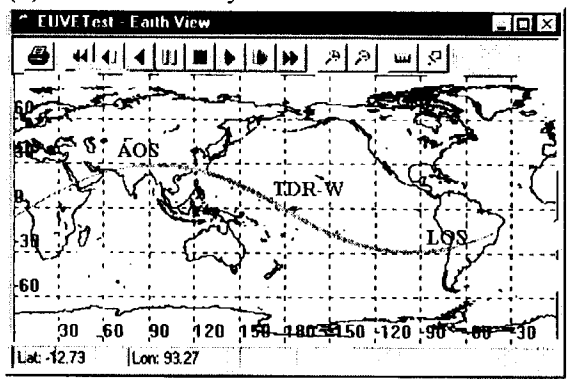

(b) Pass #3 of Day 134

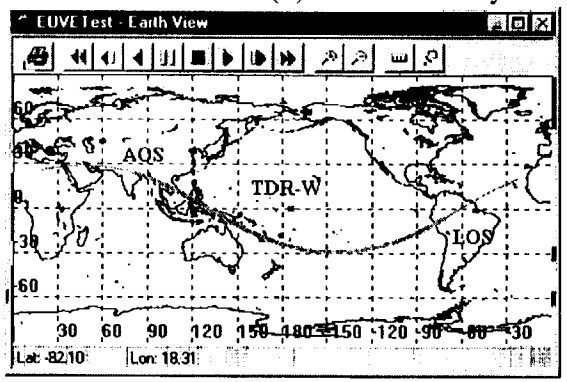

(c) Pass #1 of Day 135

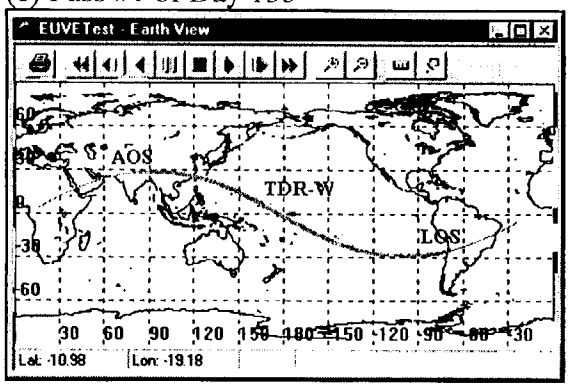

(d) Pass #2 of Day 135

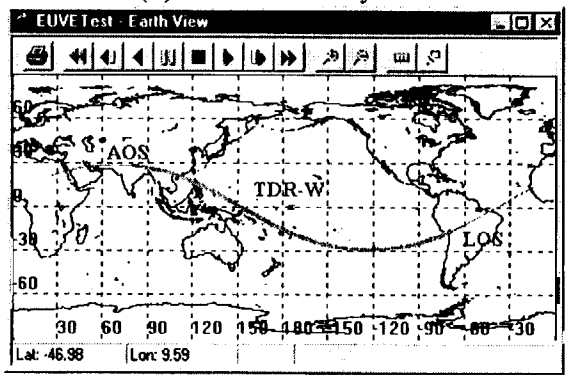

(e) Pass #3 of Day 135

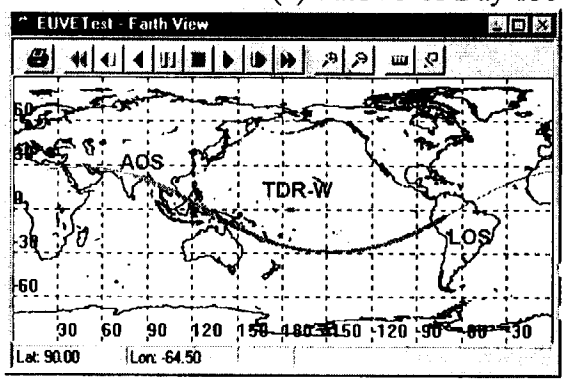

Figure 10 - Simulated EUVE Passes; EUVE Ground Track Shown as a Sinusoid with Darker Shading Indicating the Contact Region

for spacecraft antennas on inertially-stabilized satellites has a potential use in satellite communication system design.

From an inspection of the simulated azimuth and elevation angles of the TDRS with respect to the EUVE, we find that they change over the pass time by up to 7° from boresight. To investigate limits on the performance in this configuration, several test simulations beyond those used to establish minimum acceptance cone profiles were developed. The first case investigated was that of a misaligned antenna with the results illustrated in Figure 11. Here, the simulated LEO satellite antenna is offset by 5° in yaw from its optimal value. As can be seen by a gap in the coverage near -110° longitude, the full-pass coverage is not obtained. However, if the field of view is increased from ±6.2° to ±10°, the full pass coverage is again achieved as if the antenna had correct pointing. A second case considered was that of the antenna field of view being set to ±32° with optimal antenna pointing being fixed at that needed for the second orbit of a three-orbit sequence. In this case, all three orbits are covered from the one pointing position as shown in Figure 12. In this case, all three passes for the second day of testing could have been covered with a suitable broad-beam antenna.

An extended set of simulations was run to determine the effectiveness of the non-active antenna pointing over a 31-day period. In these simulations, both the TDRS East and TDRS West satellites were used as potential targets for an inertially-controlled LEO satellite. The antenna position was fixed at that for an orbit whose descending node was near the TDRS West subsatellite location. Figure 13 illustrates the average number of contacts per day as a function of the antenna acceptance cone angle. For narrow cone angles, the LEO satellite is able to make one contact per day through each TDRS. As the acceptance cone angle increases, the number of contacts per day increases through approximately three contacts per day at an antenna field of view of ±30°. As can be seen, the number of contacts per day is the same for both TDRS even though the pointing was optimized for TDRS West. In all cases, the contacts through TDRS East and West did not occur on the same orbits.

Related to the number of contacts per day is the duration of each contact. Figure 14 illustrates the average and maximum contact durations over the same 31-day simulation period used above. As can be seen, the maximum duration is approximately 60 minutes and is not a function of antenna field of view as long as the half-angle exceeds the 6.2-degree minimum. This occurs on orbits where the pointing is optimized for boresight pointing. The second part of the plot is the average contact duration which is a function of the antenna field of view. For the single contact per day with the narrow field of view, the average time is 25 minutes. For the large fields of view, the average contact duration rises to nearly 50 minutes. These results are illustrated for TDRS West and are similar for TDRS East.

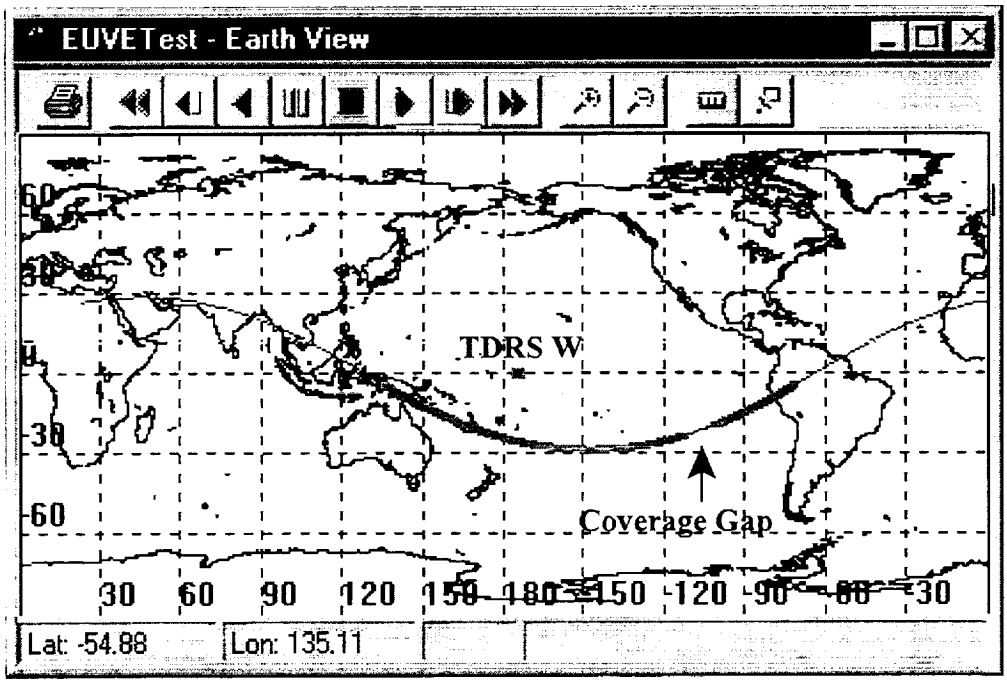

Figure 11 - Same simulated pass as #3 on Day 135 of Figure 10 but with the spacecraft off-pointed by 5° in yaw. The coverage gap occurs near -110° longitude.

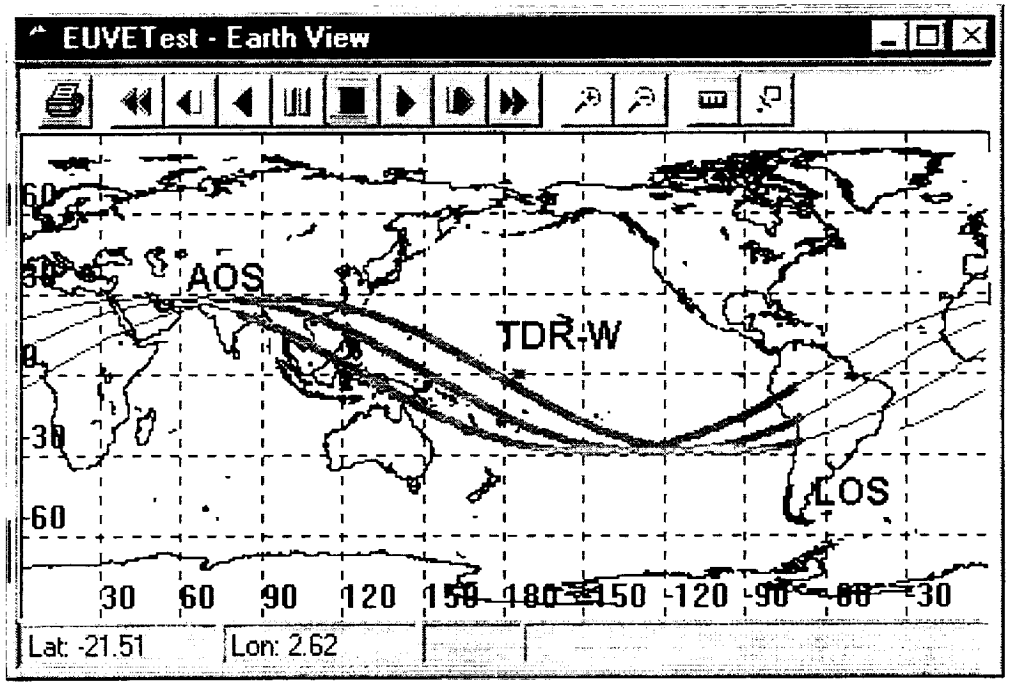

Figure 12 - Simulation of three consecutive passes for 14 May 1996 with the antenna field of view to ±32°. The thick lines represent simulated contact times.

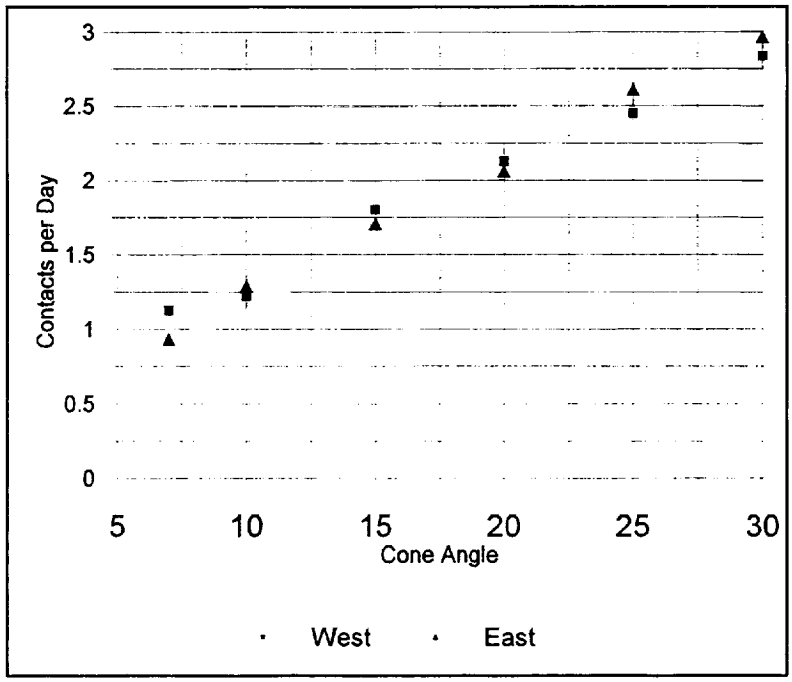

Figure 13 - Average number of contacts per day averaged over a 31-day period

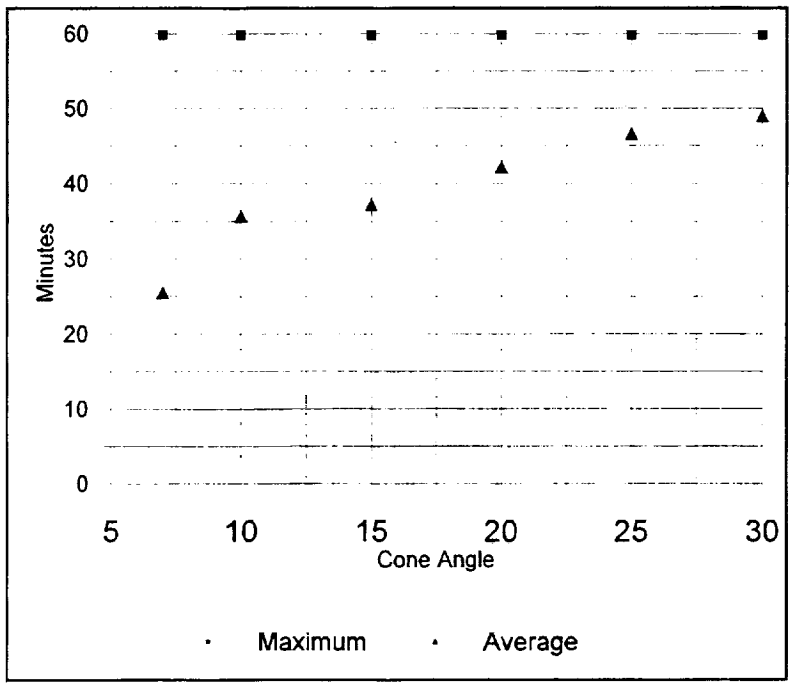

Figure 14 - Maximum and average daily contact duration over a 31-day period

SECTION 3 - EXPERIMENTAL VERIFICATION

For each type of attitude control model for the LEO satellite, we have a series of experiments conducted with orbiting satellites to give an indication of the validity of the simulation results. In these experiments, the TOPEX is used to model the nadir-pointing, spin-stabilized satellite and EUVE is used to demonstrate the effects of fixed antennas on inertially-controlled satellites.

3.1 NADIR-POINTING SATELLITE EMULATION

The experimental confirmation of the nadir-pointing results was the most difficult from an operational point of view because we needed a satellite that maintained the proper attitude control and one on which we could obtain experimental time. The Ocean Topography Explorer (TOPEX) project office was most helpful in arranging the time on this satellite.

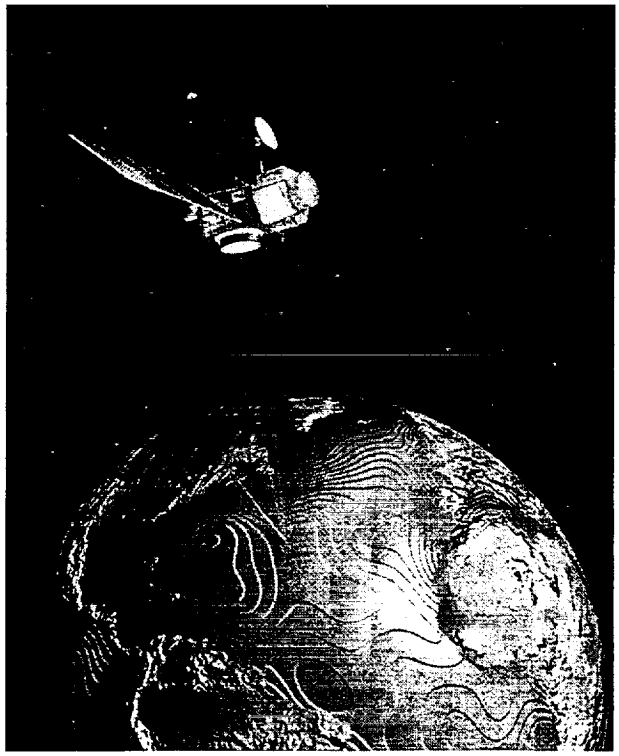

Figure 15 - TOPEX spacecraft.

3.1.1 Experiment Configuration

The pointing experiment conducted between the TOPEX satellite (see Figure 15) and the TDRS was designed to provide experimental verification to the simulation studies into the potential for non-gimbaled antennas to point at the TDRS satellites in the SN constellation and provide useful data

throughput. The test was designed to show that

1. A user satellite using a fixed-pointed antenna will be able to initiate and maintain contact with a TDRS when that antenna is pointed at the user satellite's local zenith position
2. This will occur on those orbits where the user satellite's orbit passes near the TDRS subsatellite point
3. The contact duration and data quality will be sufficient to provide a reasonable data service.

While the concept was originally developed using low-gain, non-directional antennas, this experiment was conducted with a high-gain antenna on the TOPEX. While the high-gain antenna will have a HPBW less than the beam width used in the simulation analysis, it is expected that the TOPEX system will have sufficient margin to maintain a contact even when operating on an antenna side lobe and not the antenna main lobe.

During the experiment runs, two major data sets were to be collected during the contacts between TOPEX and the assigned TDRS: signal strength indicators and data quality indicators. This data was developed at JPL based on the normal performance monitoring data supplied from the WSC to a user. In particular, the minimum data set to be collected included

1. Signal strength indication at the WSC receivers
2. An estimate of the received signal BER
3. Signal start and stop times.

JPL elected to collect other data, in particular, the forward link AGC voltage to give an indication of the forward-link signal strength.

During the experiment time, the TOPEX was configured to send a test data set on the Q channel with a data rate of 16 kbps. The times for the experiment opportunities were determined by

1. Non-interference with scheduled operations at WSC and for TOPEX
2. TOPEX passing within 20° of a TDRS subsatellite point at closest approach
3. Ability to try communications with both TDRS East and TDRS West
4. Attempt to have two passes close in time on different TDRS satellites.

The duration of the experiment was determined by the time for the TOPEX to travel the distance along its orbit corresponding to a pointing angle range of ± 20° from a given TDRS. From these general constraints, a list of potential dates and times in June 1997 were submitted to JPL for investigation of potential access times. From the general list, the dates and times listed in Table 8 were selected by JPL as experiment windows for data collection. Figures 16 through 20 illustrate the ground tracks for TOPEX, TDRS East and TDRS West during these experiment windows. The orbital ground tracks were generated at NMSU using STK. Table 9 lists the orbital elements used in the predictions.

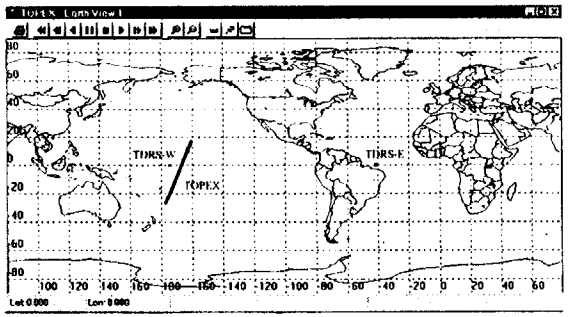

Figure 16 - TOPEX ground track for day 174 and access to TDRS-W.

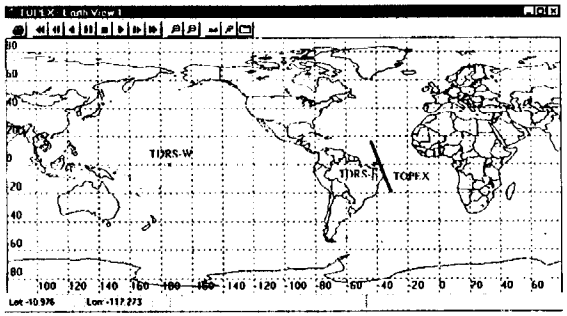

Figure 17 - TOPEX ground track for day 175 and access to TDRS-E.

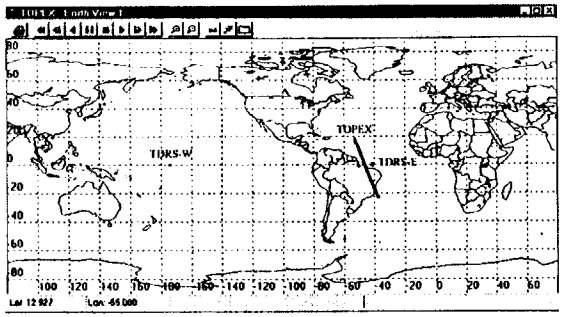

Figure 18 - TOPEX ground track for day 176 and access to TDRS-E.

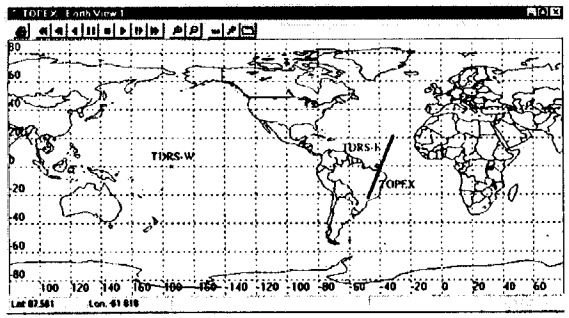

Figure 19 - TOPEX ground track for day 178 and access to TDRS-E.

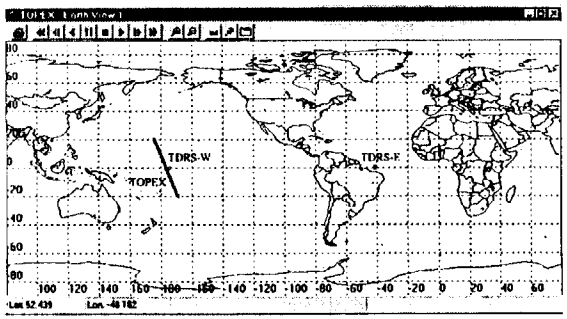

Figure 20 - TOPEX ground track for day 178 and access to TDRS-W.

Table 8. TOPEX Experiment Windows of Opportunity				
Day Number	**Date**	**Start Time**	**End Time**	**TDRS**
174	23 June 1997	3:42:30	3:55:00	West
175	24 June 1997	6:54:30	7:06:00	East
176	25 June 1997	7:15:15	7:29:00	East
178	27 June 1997	15:27:30	15:40:30	West
178	27 June 1997	18:15:30	18:29:30	East

Table 9. TOPEX and TDRS Orbital Elements			
Orbital Element	**TOPEX**	**TDRS-East**	**TDRS-West**
spacecraft identifier	22076	19883	21639
epoch	97173.53461370	97176.06688969	97176.29836412
inclination angle (degrees)	66.0378	0.6707	0.0813
eccentricity	0.0008359	0.0002370	0.0004207
Right Ascension of Ascending Node (degrees)	163.4372	85.5045	101.0808
Argument of Perigee (degrees)	278.7732	26.4777	27.5138
Mean Anomaly (degrees)	81.2337	144.3773	77.9855
Mean Motion (rev/day)	12.80930736	1.00270071	1.00274832

3.1.2 Access Time

The first check made on the experiment was to cross check the predicted pointing from TOPEX to TDRS for each pass. These pointing angles were used to estimate the start and stop times for each pass. This was given to the scheduling office for scheduling the experiment times. Figures 21 through 25 show the reported zenith angle between the TOPEX high gain antenna boresight pointing and the TDRS used for the contact. Also given is the predicted pointing angle estimated by STK. The STK analysis did not have the actual TOPEX attitude so the difference between the measured and the predicted would be expected to have an uncertainty of a few degrees. This is what is seen in these graphs. STK also generated predictions of the TOPEX azimuth pointing angle to TDRS and these can be compared with the TOPEX results but that result does not prove a reasonable accuracy

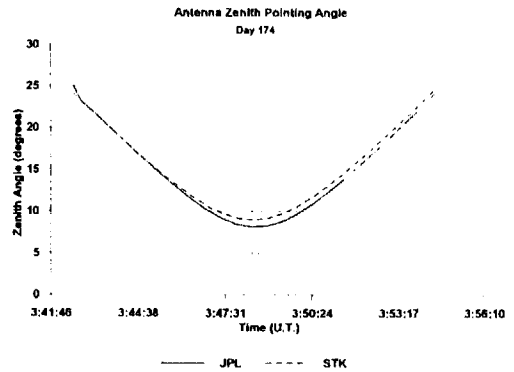

Figure 21 - TOPEX to TDRS antenna pointing relative to boresight for day174.

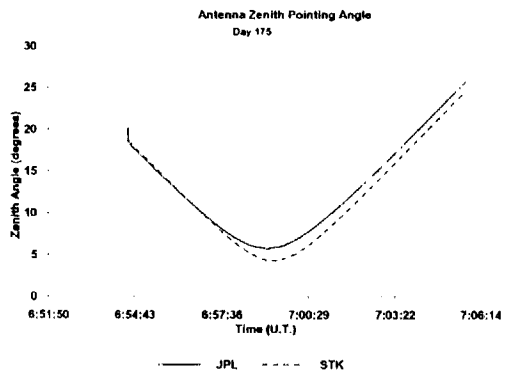

Figure 22 - TOPEX to TDRS antenna pointing relative to boresight for day175.

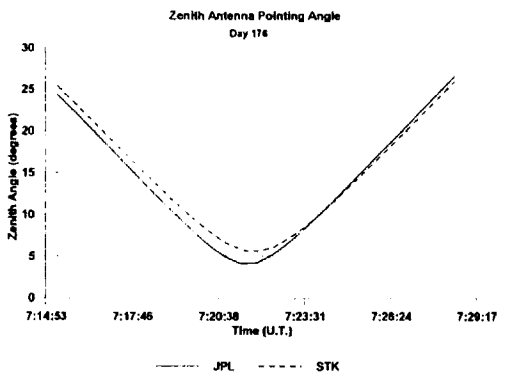

Figure 23 - TOPEX to TDRS antenna pointing relative to boresight for day176.

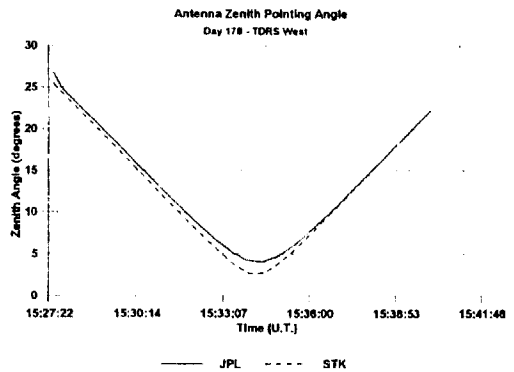

Figure 24 - TOPEX to TDRS antenna pointing relative to boresight for day178.

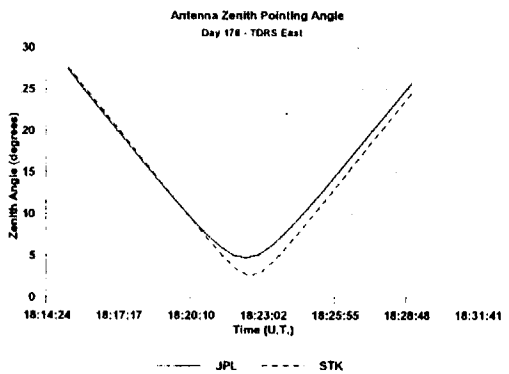

Figure 25 - TOPEX to TDRS antenna pointing relative to boresight for day178.

check because the TOPEX attitude in true, three-dimensional space was unknown to the experimenters at NMSU and, therefore, there is a considerable angular offset between the STK results and the TOPEX data.

The predicted access times for each pass were generated prior to the experiment window based on when the TOPEX would enter or leave the 20-degree circle around the TDRS subsatellite point. The pass durations were chosen to be approximately 10 minutes (see Table 8) with the expectation that we would observe the receiver lock-up process at the WSC. The return link from TOPEX through TDRS receiver lock status is indicated in Figures 26 through 30 where a value of 0 indicates receiver lock while a value of 2 indicates that the receiver is not locked. The plots generally indicate a main region of receiver lock around the center of the pass time and a shorter region on either side of this where the receiver has short lock periods. Table 10 gives the return link primary access regions and an indication of secondary access regions for each pass. Table 11 gives the total time in each region. There was not a similar measurement available for the forward link to TOPEX through TDRS.

Table 10. TOPEX Return Link Access Times Based on Receiver Lock Status

Pass Day	Primary Start	Primary Stop	Secondary Start	Secondary Stop
174	3:45:35	3:52:19	3:53:05	3:54:19
175	6:55:45	7:05:09	7:05:40	7:06:00*
176	7:18:25	7:25:09	7:27:05	7:27:54
178-W	15:31:05	15:37:59	15:28:05 15:39:25	15:30:44 15:40:25*
178-E	18:19:00	18:26:24	18:16:45 18:27:55	18:17:39 18:29:19

* scheduled end of pass time

3.1.3 Data Quality

The estimated Bit Error Rate (BER) performance of the data sets is illustrated in Figures 31 through 35. This data is derived from ODM data for the TOPEX Q channel and was supplied from the WSC. As can be seen from these plots and the receiver lock status plots, when the receiver was in lock, the BER generally was at the 8 level corresponding to an estimated maximum BER of 10^{-8}.

The antenna pattern and the change in the link distance over the pass time are expected to modify the observed signal strengths from that seen in boresight alignment at closest approach between the TOPEX and the TDRS. These effects would be observable on both the forward and return data links through TDRS to the TOPEX. In this section, we will outline the expected contributions of both of these effects.

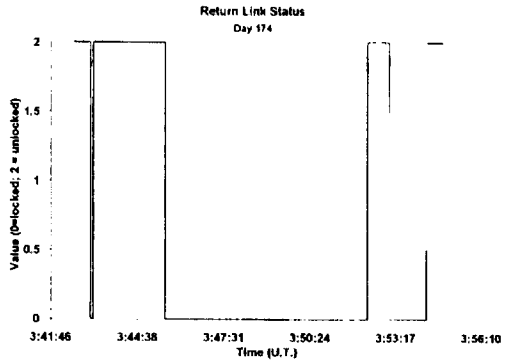

Figure 26 - Receiver lock status at the WSC for day 174.

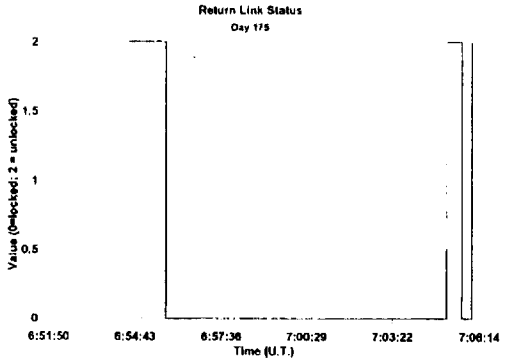

Figure 27 - Receiver lock status at the WSC for day 175.

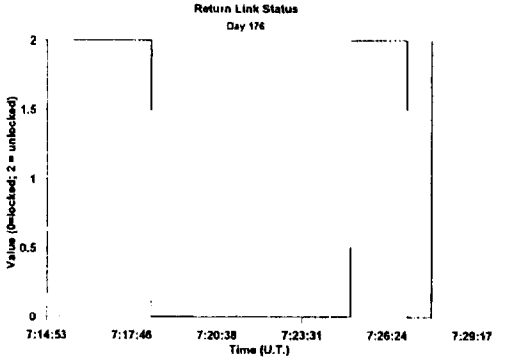

Figure 28 - Receiver lock status at the WSC for day 176.

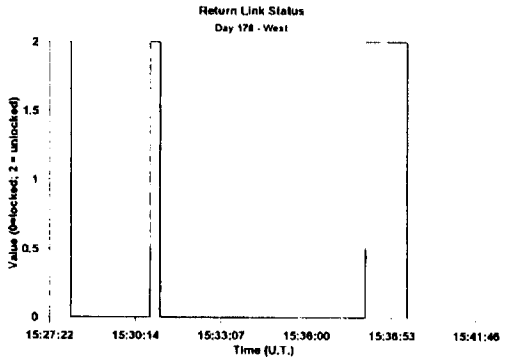

Figure 29 - Receiver lock status at the WSC for day 178 and TDRS West.

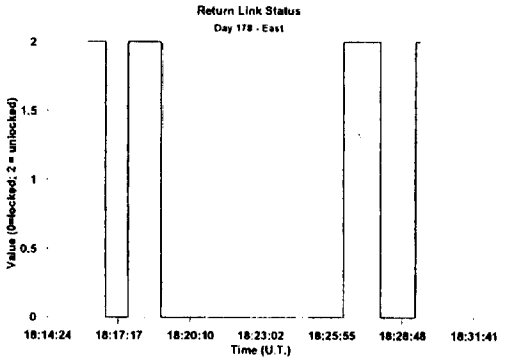

Figure 30 - Receiver lock status at the WSC for day 178 and TDRS East.

Table 11. TOPEX Return Link Access Durations		
Pass Day	**Primary Duration (minutes)**	**Secondary Duration (minutes)**
174	6.73	1.23
175	9.40	0.33*
176	6.73	0.82
178-W	6.90	2.65, 1.00*
178-E	7.40	0.9, 1.40

* terminated by scheduled end of pass

The antenna pattern will exhibit relative gain variations because we have fixed the pointing of the TOPEX antenna towards the local zenith. Normally, this antenna would be tracking the relative TDRS position and provide close to boresight pointing for the data service. In this experiment, the TOPEX will suffer a considerable pointing loss towards the TDRS directions because the tracking has been disabled. We can estimate the size of the pointing loss by approximating it with a symmetrical pattern and use the following relationship for the pointing loss, L_p, [16],[17]:

$$L_p = 64\left|\frac{J_2(u)}{u^2}\right|^2$$

where $u = sin(\theta)\lambda/D$ given that θ is the pointing angle from boresight (the same angles as plotted in Figures 21 through 25), λ is the radiation wavelength corresponding to a carrier frequency of 2287 MHz, and D is the TOPEX antenna diameter of 1.29 meters [18].

The space loss, L_s, effect can be computed from

$$Ls = (4\pi R/\lambda)^2$$

where λ is the radiation wavelength and R is the link distance.

When working in dB units, both losses can be added together for a combined expected loss value. In Figures 36 through 40, the relative value of the combined loss is plotted. This is the difference in dB between the computed loss at every moment in time through the pass and the minimum loss occurring at the mid-point of the pass. As can be seen for each pass, there is a central lobe centered near the mid-pass point and several side lobes. The side lobes arise from the antenna pattern. The space loss provides a nearly-constant offset because the range does not change substantially over the 10-minute pass.

We can estimate the HPBW of the TOPEX high-gain antenna by [19]

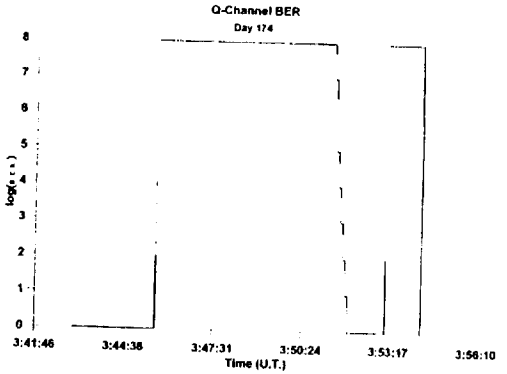

Figure 31 - Q-Channel BER Status for day 174.

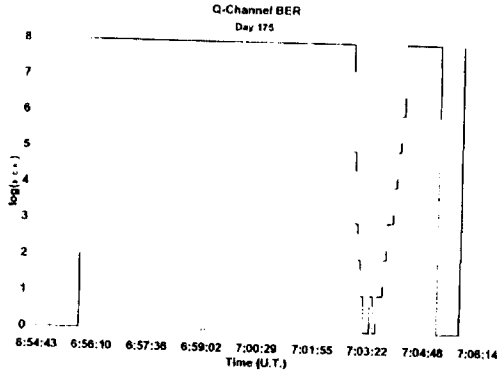

Figure 32 - Q-Channel BER Status for day 175.

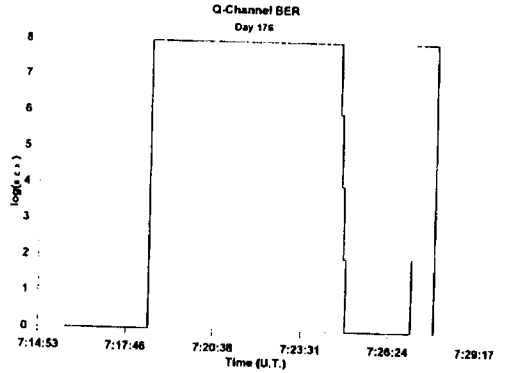

Figure 33 - Q-Channel BER Status for day 176.

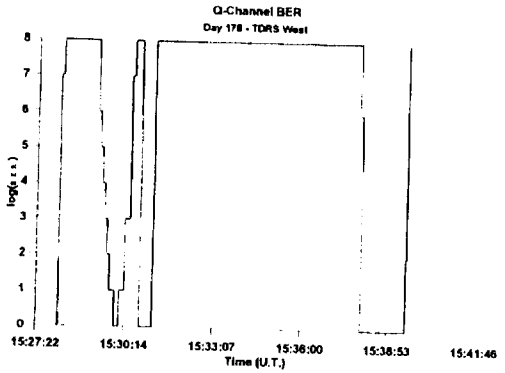

Figure 34 - Q-Channel BER Status for day 178 and TDRS West.

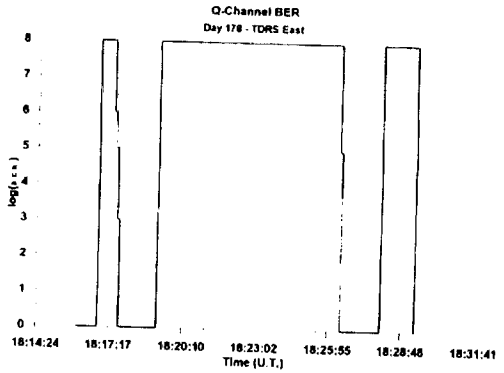

Figure 35 - Q-Channel BER Status for day 178 and TDRS East.

$$\text{HPBW} = \frac{72.8^{\circ}\ \lambda}{D}$$

where D is the antenna diameter of 1.29 meter and λ is the wavelength of 0.131 meter. The initial predictions were made assuming an antenna filed of view of $\pm 40^{\circ}$. The actual TOPEX antenna has a HPBW of 7.4°. Based on the more restrictive HPBW than the initial analysis was expecting, the indicated lock status would be expected to cover a more narrow range in time than that observed. By comparing the lock status plots shown in Figures 41 to 45 with the predicted relative signal strength plots, we observe that the lock times cover the main antenna lobe and most of the first side lobe on either side of the main lobe. Typically, the receiver falls out of lock around the time of the second null in the antenna pattern.

The integrated receiver signal strength remained high during the period when the receiver at the WSC was in lock. During these periods, the estimated BER was on the order of 10^{-8}. This indicates that the system has sufficient margin to produce a reliable output even when the received signal strength varies by several dB. This leads us to hypothesize that the expected performance for systems using this method of TDRS access would be better than that limited to access times within the HPBW alone.

3.2 INERTIALLY-STABILIZED SATELLITE

As was mentioned earlier, the EUVE was used in an attempt to emulate the sweeping motion of a nadir-pointed satellite. The EUVE used a fixed antenna during each pass. We did not find it to be a good analog of the desired motion. However, we did find it had the ability to provide performance near that of a tracking antenna even with the antenna properly fixed in position.

3.2.1 Experiment Configuration

The objective of this test was to demonstrate that large quantities of telemetry data can be transmitted from the EUVE spacecraft via TDRS using a fixed, zenith-pointed spacecraft antenna. To emulate the action of a fixed, zenith-pointing spacecraft, the Flight Dynamics Facility at NASA's Goddard Space Flight Center suggested pointing the EUVE antenna to the correct position to directly point to TDRS as the EUVE passed directly under the TDRS. This antenna pointing would be maintained during the duration of each pass and then changed appropriately for each pass. The test was run at the times indicated in Table 12.

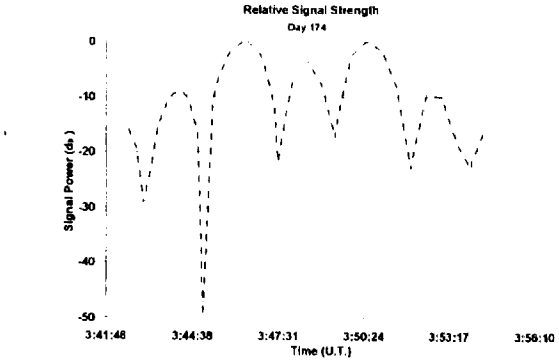

Figure 36 - Pointing loss and space loss for day 174.

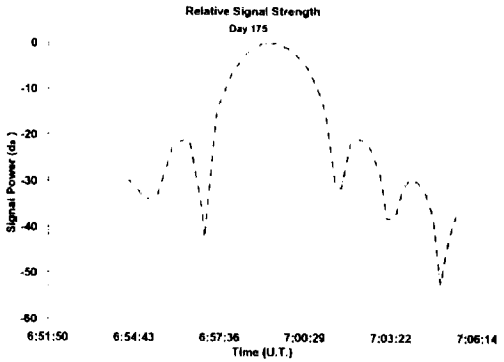

Figure 37 - Pointing loss and space loss for day 175.

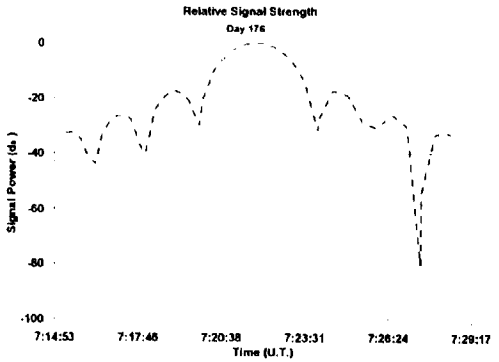

Figure 38 - Pointing loss and space loss for day 176.

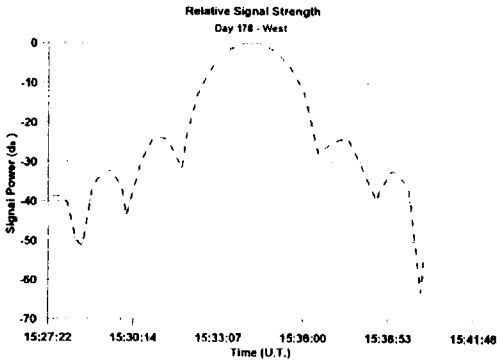

Figure 39 - Pointing loss and space loss for day 178 and TDRS West.

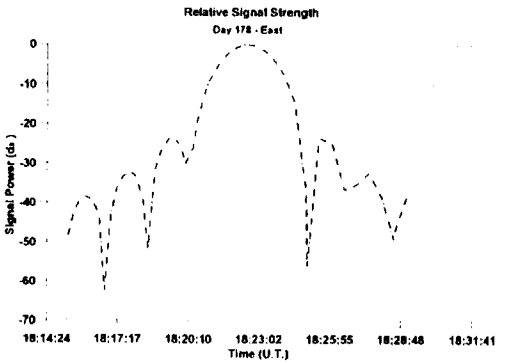

Figure 40 - Pointing loss and space loss for day 178 and TDRS East.

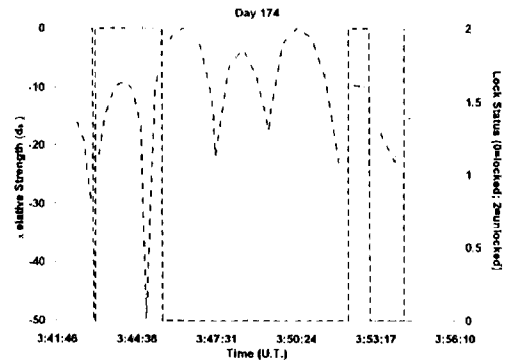

Figure 41 - Correlation of the signal strength with the receiver lock status for day 174

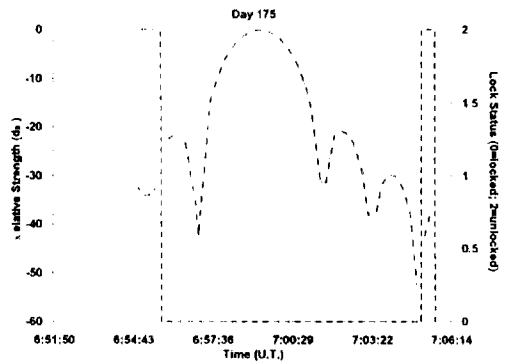

Figure 42 - Correlation of the signal strength with the receiver lock status for day 175

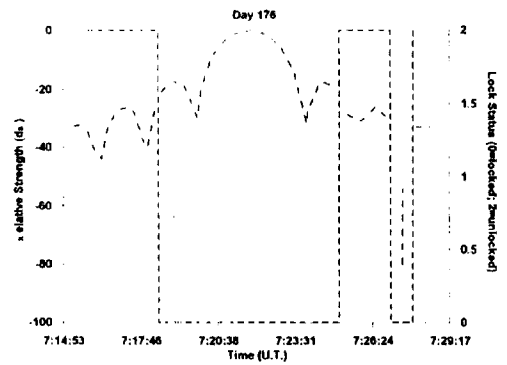

Figure 43 - Correlation of the signal strength with the receiver lock status for day 176

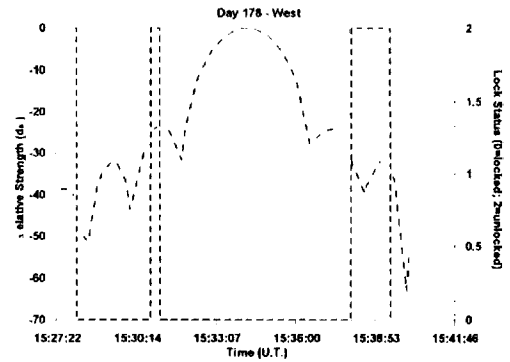

Figure 44 - Correlation of the signal strength with the receiver lock status for day 178 and TDRS West

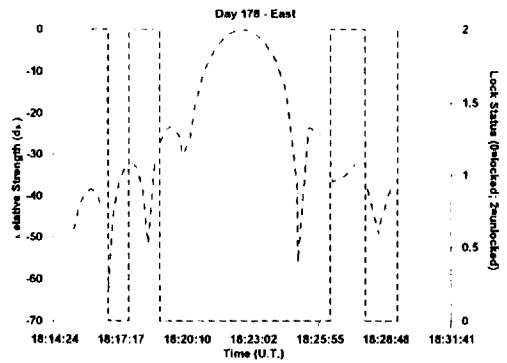

Figure 45 - Correlation of the signal strength with the receiver lock status for day 178 and TDRS East

Table 12. EUVE Test Times		
Date	**DOY**	**Hours (U.T.)**
13 May 1996	134	12:09 - 16:02
14 May 1996	135	11:47 - 15:41

During the experiment data collection times, the EUVE POCC commanded the spacecraft to point at zenith and then transmitted a test data pattern at DG1 Mode 2 dual-channel configuration. The I Channel data rate was 1 kbps and the Q Channel data rate was 32 kbps.

As developed in [20], the test configuration would be as follows for the ground equipment:

1. EUVE data would be returned to the WSC via the MA return data stream.
2. Data would be demodulated using one of the available Integrated Receivers and both the I and Q Channel would be received.
3. The baseband data would be routed through the Low Rate Black Switch to the Multiplexer for packaging in 4800-bit blocks and time-tagging of the data.
4. The output of the Multiplexer would be transmitted to the EUVE POCC via NASCOM
5. The Multiplexer output would also be routed to the Demultiplexer where the EUVE Q Channel data would be removed.
6. The Q Channel data would be transmitted over a RS-422 link to a NASCOM Interface Board resident on a PC supplied by NMSU.
7. The PC would be used as a data collection PC for the Q Channel data. This PC would also have access to a telephone line so the data could be transmitted to the NMSU campus.

Additional test equipment used during the tests was an oscilloscope to monitor data connections at the WSC during each pass.

Based on the simulations, it was expected that the following results would occur with this set of tests:

1. Each EUVE pass will last for approximately five minutes centered on the time when the EUVE passes directly under the TDRS; this will be a function of the dynamic range of the receivers based on their pre-pass estimated best settings with a few minutes longer being possible if conditions act favorably.
2. The signal should fall off quickly outside of this time because the EUVE antenna system has a relatively high gain compared with the situation this concept was designed for.
3. We should be able to determine how quickly the receivers can lock onto the signal as it sweeps in view of the TDRS.

While this is not an exact analog of the spin-stabilized platform that the concept was designed for, it was expected to exhibit behavior close enough to validate the concept.

3.2.2 Access Time

During the test passes, the expected access time was predicted to be approximately five minutes centered on the time when EUVE was closest to TDRS West. Because the EUVE antenna system has a significant gain and a correspondingly narrow antenna pattern, an accommodation was needed to make the test similar to that predicted to be found with a broad-beam antenna sweeping past the TDRS location. To accomplish this, the EUVE control center pointed the spacecraft antenna to the TDRS position at the time of closest approach and fixed it there for the pass duration. This pointing was done prior to the start of the pass and active pointing during the pass was disabled by ground command. During the test passes, it was expected that, as EUVE moved along its orbit, it would sweep past the TDRS position and emulate the desired contact profile.

The results of these test contacts were that the contact times greatly exceeded the predicted value of five minutes. To allow for timing uncertainties and to allow for tracking of the receiver acquisition process, data were collected for a period of 30 minutes centered around the expected contact mid-point. The actual experiment was able to collect data over the entire experiment period and not just the short duration around mid-pass.

3.2.3 Data Quality

The data gathered consisted of EUVE data files, and ground station receiver estimates of the signal energy per bit to noise density, E_b/N_o, and EUVE Doppler offset. The received E_b/N_o for these passes is illustrated in Figure 46 (pass #2 had no data recorded due to configuration checks). Instead of a gradual acquisition and loss process at the start and end of the data acquisition interval during each pass, the ground station receivers immediately locked onto the EUVE communications signal relayed through TDRS at the scheduled start of the communications service time and stayed locked until the scheduled end of the service time.

During the six data collection passes between EUVE and TDRS West, it was noticed that the estimated the energy-per-bit to noise density ratio, E_b/N_o, as measured at the ground station receiving equipment, varied by several dB. Using the same analysis technique for antenna pointing loss and space loss as was done with TOPEX to better understand the E_b/N_o results, we estimated the space loss and antenna pattern contributions to the link as a function of the small variations in pointing during a pass. The variation in the received E_b/N_o should be a function of two effects: the changing distance between the LEO satellite and the relay satellite due to orbital motion and the changing gain in the LEO satellite antenna because the relay satellite is not always aligned with the antenna boresight pointing.

The predicted variation in the received E_b/N_o is based on the addition of the space loss and antenna pattern loss in dB units over time and is illustrated for each pass in Figure 47. This can be compared with the observed measurements as shown in Figure 48 which illustrates the normalized, predicted and observed E_b/N_o attenuation for all passes in the series. In most cases, the agreement is to within

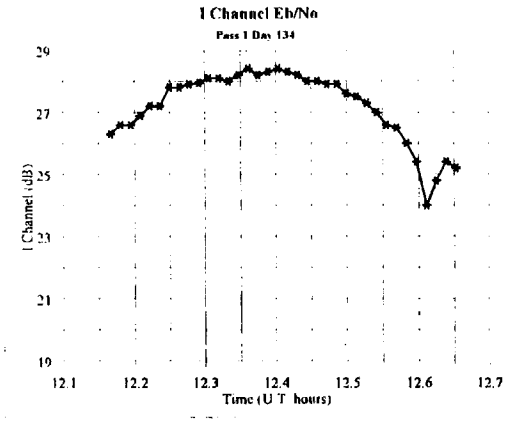

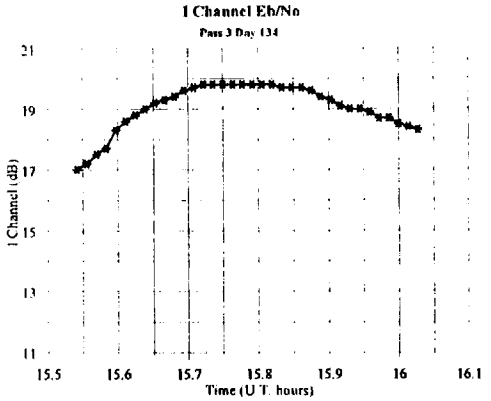

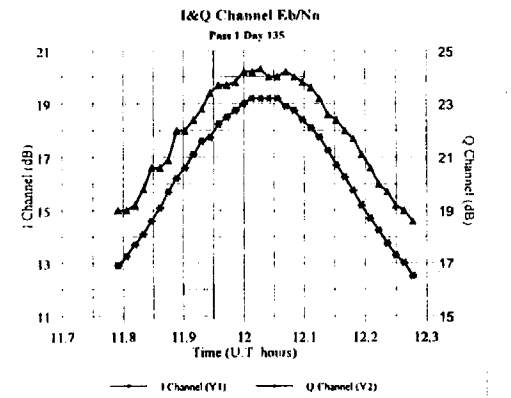

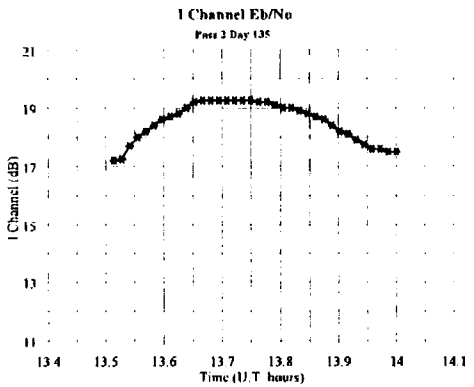

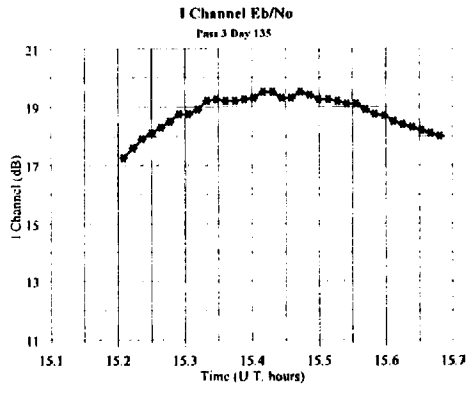

Figure 46 - E_b/N_o measurements for each EUVE pass as measured at WSC.

1 dB. During the observed contact time, the space loss typically accounts for approximately 1 dB of the total signal variation while the antenna pattern gain variation accounts for the rest. Over the whole simulated contact time, the total variation in E_b/N_o is predicted to be approximately 6 dB with the space loss amounting to approximately 2 dB of the variation and the antenna pointing loss contributing the remainder. Because we are inferring the EUVE attitude and antenna pointing within the simulation and do not have access to the actual pointing vectors and spacecraft attitude, we expect there to be some variations between the predicted signal variations and the actual measurements. Also, no special care was taken at the WSC to calibrate the measurement devices for exact E_b/N_o measurements so some variation is expected here as well. Given these uncertainties, we find this level of agreement to be reasonable for this experiment configuration.

(a) Pass #1, Day 134

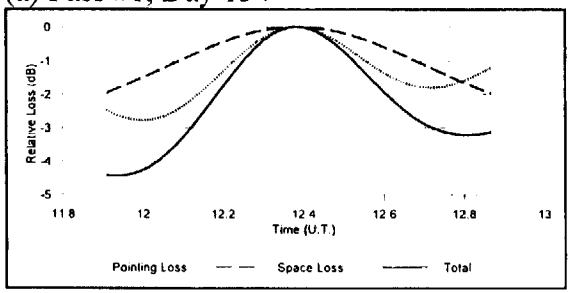

(b) Pass #3, Day 134

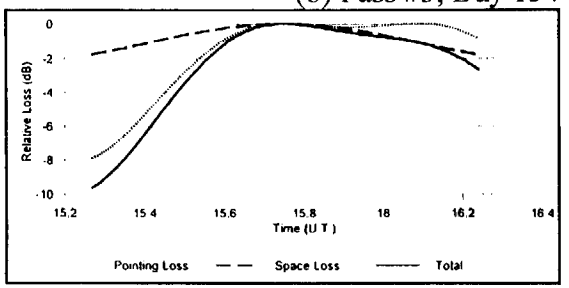

(c) Pass #1, Day 135

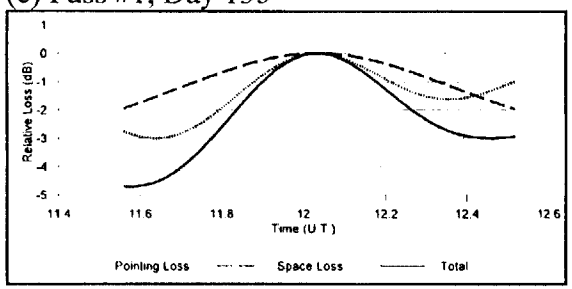

(d) Pass #2, Day 135

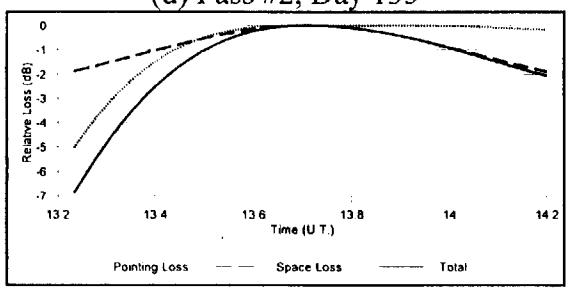

(e) Pass #3, Day 135

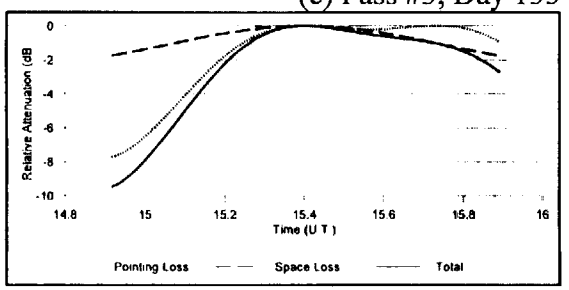

Figure 47 - Predicted Pointing Loss and Space Loss Variations over the Simulated Contacts

(a) Pass #1, Day 134

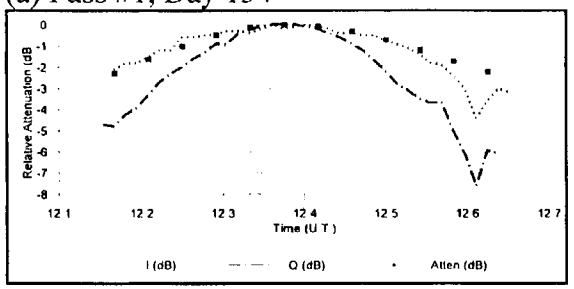

(b) Pass #3 Day 134

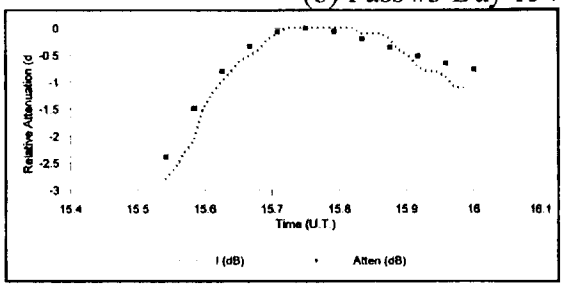

(c) Pass #1, Day 135

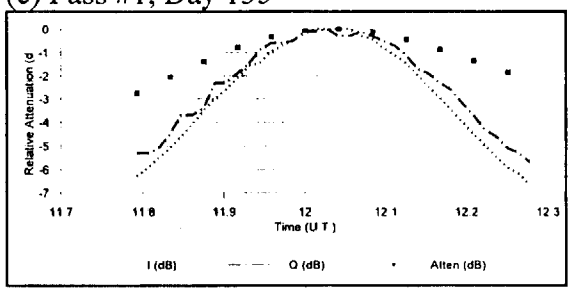

(d) Pass #2, Day 135

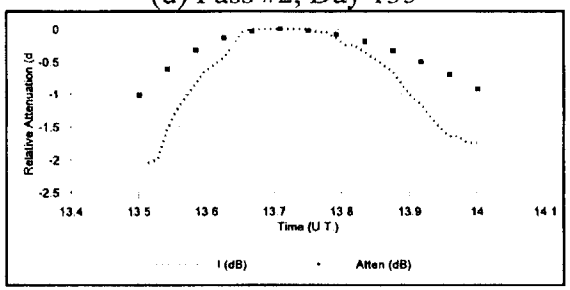

(e) Pass #3, Day 135

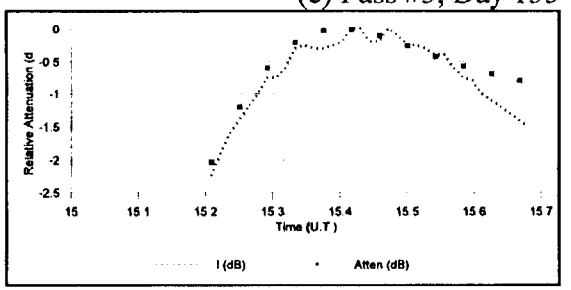

Figure 48 - Predicted and Observed Signal Variation over the Contact Duration

SECTION 4 - APPLICATION OF RESULTS

4.1 PREDICTED DATA THROUGHPUT THROUGH TDRS

The contact times through a given TDRS or the entire constellation are only one part of the solution to the problem of small satellite access of the SN. The other part of the solution comes from examining the required data throughput and the baseline communications system design to determine if they are compatible and achievable. In this section, we will look at the two ways to approach the solution. The first takes a given system transmission configuration and EIRP and determines what is the available data throughput. The second takes the data throughput requirements and works back to determine the system communications requirements to support it.

Common to both analysis methods is the computation for the link power budget through the TDRS in the SN. The analysis requires the slant path found from the simulations. Based on design information given in [21], the expected data rate, R_d, for a TDRS S-band multiple access service can be computed from

$$R_d\ (dBbps) = EIRP - M + K + L_s + L_{pol} + L_{pnt} + L_{nc} + L_{rfi} \quad (1)$$

where M is the link margin, L_s is the space loss, L_{pol} is the antenna polarization loss, L_{pnt} is the antenna pointing loss, L_{nc} is the system noncompliance loss, and L_{rfi} is the RFI margin (all losses and margins are in dB units). The units on the data rate are *10log(bps)* or *dBbps*. The constant K is a service-specific parameter and equals 221.8 dB for a SN multiple access service with a worst-case bit error rate of 10^{-5} when the data are convolutionally coded with a standard rate ½ and constraint length 7 code (this is a standard NASA communications configuration when using the SN). To determine the maximum transmission rate possible, we will assume that the link margin and the polarization, pointing, noncompliance, and RFI losses are 0 dB. The space loss is estimated using [21]

$$Ls\ (dB) = -(32.45 + 20\ log(R) + 20log(f)) \quad (2)$$

where R is the slant range in kilometers and f is the multiple access transmission frequency of 2287.5 MHz. The link margin, M, is taken to be at most 3 dB corresponding to the maximum margin required within the antenna HPBW. Naturally, if the system is able to supply a larger margin, then the contact duration can be extended to the limit of the useful margin provided in the design.

4.1.1 Throughput Prediction Based on Constant Power Level

The above relationships were used to generate a listing of potential data rates as a function of satellite EIRP and slant range with the results given in Table 13. In making the computations, we are assuming the baseline communications system configuration with the nadir-pointing, spin stabilized satellite. Taking the baseline power assumption with a typical helical antenna as described

Table 13. SN Available Data Rates as a Function of EIRP and Slant Range with 0 dB Link Margin and 0 dB Implementation Loss		
	Data Rate (bps)	
Slant Range (km)	EIRP = 15 dBW	EIRP = 19.3 dBW
35000	42476	114325
35200	41995	113030
35500	41288	111127
35700	40826	109866
36000	40149	108062
36500	39056	105122
36700	38632	103979
37000	38008	102300
37500	37001	99590

in Section 5, we start the computation with an expected satellite EIRP of 21.3 dBW on-axis. The 5-turn helix antenna has an expected HPBW of 55° which would allow up to 22.5° of off-axis pointing to stay within a 3-dB margin. Allowing for a maximum 20-degree off-axis pointing to correspond with the simulations, we reduce the antenna's gain by 2 dB to account for this which gives an EIRP of 19.3 dBW. The analysis was also performed with a more realistic design estimate for total system losses (internal component losses, polarization mis-match loss, etc.) amounting to 4 dB and subsequently the EIRP was reduced to 15 dBW. No other losses were assumed at this point without having actual candidate hardware for a spacecraft. The results in Table 13 are then a realistic upper limit for the achievable data rates. In analyzing the 45-degree half-angle case, we assume that an EIRP of only 15 dBW will normally be available from the nadir-pointing, spin-stabilized satellite, although performance is given for the 19.3 dBW case as a comparison if an alternative technology is used. This is because a helical antenna would need to be operated considerably off-axis to support the broad pointing angles.

The maximum slant paths for the various orbital configurations are given in Table 14 with a typical value being 36000 km. These maximum slant paths correspond to the edges of the service support window and will be used to set the data rate for the pass. In actuality, during any satellite service support time, the slant path to a TDRS will vary through the pass and will be minimal at the mid-point of the pass and highest at the end points of the pass (pass start and stop times). The pass maximum path length then sets a worst-case slant path length and the lowest data rate assuming that the data transfer rate is kept constant during the pass. As the path becomes shorter, the data rate

Table 14. Spin-Stabilized-Satellite-to-TDRS Maximum Slant Paths				
		Orbital Altitude		
Pointing Half-Angle	Inclination Angle	600 km	900 km	1200 km
20°	28.5	35561 km	35529 km	35077 km
20°	sun-synch	36561 km	35263 km	34976 km
45°	28.5	36958 km	36720 km	36482 km
45°	sun-synch	36948 km	36718 km	36479 km

remaining constant has the effect of reducing the channel bit error rate thereby making the link more reliable in the middle region of the service window.

We can estimate the total daily data volume desired to be transmitted through the space network over the range of small-satellite missions at 10 kbps. This corresponds to a total production of 864,000,000 bits per day. The required minimum data rate necessary to transport this desired data volume is a function of the contact duration per day and the supported data rate for the communications system. In general, we see that narrow pointing angles from a narrow-HPBW antenna capable of supporting a relatively high data rate and only a few contacts with the SN each day can be traded against a low-gain, wide-HPBW antenna, and therefore a relatively low data rate system which has many contacts per day. For a given maximum number of total contact minutes per day that may be dictated by operational considerations, it may be possible to have a higher data throughput by using a high-gain communications system with a few daily contacts than by using a low-gain antenna with more daily contacts. With the number of contacts per day and the data rate that can be supported determined, we can estimate if any configuration provides support at the desired daily data throughput level. The daily throughput is computed by multiplying the average daily contact duration by the data rate determined from the maximum slant path for the orbital altitude and pointing angle. Sample results are given in Tables 15 through 18 for single-TDRS contacts and full SN constellation results at 15 dBW and 19.3 dBW EIRP. In each table, the total daily throughput is given as a function of orbital altitude and orbital inclination angle. From these tables, we can see that a single TDRS within the Space Network cannot give the required coverage time to support users up to the 50^{th}-percentile level when the spin-stabilized satellite has an EIRP of 15 dBW and a SMA service is used. At this lower EIRP, a long contact time through the entire SN constellation from a wide half-angle antenna is required to give the desired data throughput when a SMA service is used as seen in Table 16. If we have the higher EIRP available, then we can achieve the desired throughput by using either a wider half-angle antenna and a single TDRS or a narrow half-angle antenna and the full constellation as seen in Tables 17 and 18. The exact choice will need to be determined in the context of a specific mission model for the satellite.

A fixed ground station can usually achieve this same throughput with lower EIRP or with a higher

Table 15. Contact Duration and throughput for TDRS-W as a function of orbital altitude, inclination angle, and antenna half-angle when the EIRP is 15 dBW.								
	TDRS-W Contact Duration (min.)				Throughput (Mbit/day)			
	Orbital Inclination				Orbital Inclination			
	28.5°		sun-synchronous		28.5°		sun-synchronous	
	Half-angle		Half-angle		Half-angle	Half-angle	Half-angle	Half-angle
altitude (km)	20°	45°	20°	45°	20°	45°	20°	45°
600	43.3	264.2	19.6	105.3	107	603	49	240
900	42.1	260.7	19.6	104.4	104	604	49	242
1200	40.5	258.0	19.4	103.3	103	605	49	241

Table 16. Contact Duration and throughput for a three-TDRS constellation as a function of orbital altitude, inclination angle, and antenna half-angle when the EIRP is 15 dBW.								
	TDRS Constellation Contact Duration (min.)				Throughput (Mbit/day)			
	Orbital Inclination				Orbital Inclination			
	28.5°		sun-synchronous		28.5°		sun-synchronous	
	Half-angle		Half-angle		Half-angle	Half-angle	Half-angle	Half-angle
altitude (km)	20°	45°	20°	45°	20°	45°	20°	45°
600	126.1	784.3	59	315.9	312	1789	146	720
900	123.4	774.7	57.9	313.1	306	1796	146	726
1200	121.1	766.1	58	308.7	309	1795	148	723

data rate because of the lower space loss involved in transmitting to a fixed ground station. However, a direct comparison cannot be made without specifying a combined antenna and receiver system so that the link budget can be determined for a candidate system. In this study, we are bounding the parameters necessary to achieve the desired throughput without resorting to a proprietary ground station.

In this analysis, we are constraining ourselves to fixing the data rate to give the desired bit error rate at the edges of the coverage area which also corresponds to the highest space loss on the communications link. This occurs because we fix the slant range in equation 2 to the maximum range for a given contact. Because the actual space loss will vary over the contact time, we can look to variable-

Table 17. Contact Duration and throughput for TDRS-W as a function of orbital altitude, inclination angle, and antenna half-angle when the EIRP is 19.3 dBW.								
	TDRS-W Contact Duration (min.)				Throughput (Mbit/day)			
	Orbital Inclination				Orbital Inclination			
	28.5°		sun-synchronous		28.5°		sun-synchronous	
	Half-angle		Half-angle		Half-angle	Half-angle	Half-angle	Half-angle
altitude (km)	20°	45°	20°	45°	20°	45°	20°	45°
600	43.3	264.2	19.6	105.3	289	1622	131	646
900	42.1	260.7	19.6	104.4	281	1626	133	651
1200	40.5	258.0	19.4	103.3	278	1627	133	650

Table 18. Contact Duration and throughput for a three-TDRS constellation as a function of orbital altitude, inclination angle, and antenna half-angle when the EIRP is 19.3 dBW.								
	TDRS Constellation Contact Duration (min.)				Throughput (Mbit/day)			
	Orbital Inclination				Orbital Inclination			
	28.5°		sun-synchronous		28.5°		sun-synchronous	
	Half-angle		Half-angle		Half-angle	Half-angle	Half-angle	Half-angle
altitude (km)	20°	45°	20°	45°	20°	45°	20°	45°
600	126.1	784.3	59	315.9	841	4814	393	1939
900	123.4	774.7	57.9	313.1	823	4833	393	1953
1200	121.1	766.1	58	308.7	831	4832	398	1947

rate coding techniques as being potentially useful to make the data transmissions more efficient. This analysis was also constrained by using the SMA communications service on the SN. This is the lowest-performance communications service of the three service types available on the SN. The S-band Single Access (SSA) communications service has the next-higher performance level in the system. Referring back to equation 1, the service-specific constant, K, is 230.7 dB for an SSA service [2] versus 221.8 dB for an SMA service. This difference of 8.9 dB implies that we have the potential to trade higher data rates, shorter access times, and system availability to achieve the optimum mission model by using both the SMA and SSA communications services.

The contact times for an individual TDRS or the entire SN constellation will need to be balanced against operations constraints. While the ±45° antenna filed of view may give up to 4.8 Gbit of data throughput per day, it also requires 770 minutes per day of contact time. This service duration may be operationally unacceptable in scheduling the SN when trying to accommodate higher-priority users. Operationally, the narrow-pointing case is expected to be easier to realize in the SN scheduling system than the broader-pointing case. This indicates that a preferred mode for operating the system will be to efficiently use a short contact time with a high-gain antenna rather than depending upon a low-gain antenna with a long contact potential that cannot be realized in the actual network.

4.1.2 EIRP Required Based on Constant Throughput Level

An alternative way of casting the throughput problem is to fix the required daily throughput and then determine the necessary EIRP to accomplish the mission. To perform such an analysis, we recast Equation 1 as

$$EIRP = R_d(dBbps) + M - K - L_s - L_{pol} - L_{pnt} - L_{nc} - L_{rfi} \quad (3)$$

As before, we make the margin, M, and loss terms other than the space loss term, L_s, equal to 0 dB. The required data rate is a function of the contact time. Figure 49 illustrates the relationship between total contact time per day and the required data rate to transport 864 Mbits. For the purposes of analysis here, we will use the worst-case distance of 37000 km (the best-case distance of 35000 km makes less than 1 dB difference in the result). Given these results, Figure 50 illustrates the required EIRP for the satellite to support the desired 10-kbps equivalent throughput for the communications system. In both Figures 49 and 50, we have not distinguished between single-TDRS contacts and full-constellation contacts nor have we included the HPBW for the antenna. However, Table 19 lists required data rates and EIRP for typical single-TDRS and 3-TDRS constellation contact times. In section 4.3, we will look at potential mixes of antenna parameters and transmitter power levels required to give this minimum EIRP to support the data transport.

4.2 EXPECTED DATA THROUGHPUT BASED ON THE TOPEX EXPERIMENT

The expected data throughput based on the TOPEX experiment is based on the parameters provided by the JPL and the link analysis methodology provided in the SNUG [21]. The TOPEX EIRP computation is given in Table 20. This will be compared with the transmission requirements given in the SNUG for a BER of 10^{-5}. The data transmission rate for the entire experiment was fixed at 16 kbps on the Q channel. As we saw above, when the receiver was locked, there were essentially no data errors. This leads to the speculation that a higher data rate could have been supported in these experiments.

From the STK simulations, we determined that the maximum path distance during the TOPEX experiment was 36,000 km. This is shorter than the maximum path length typically used in SN

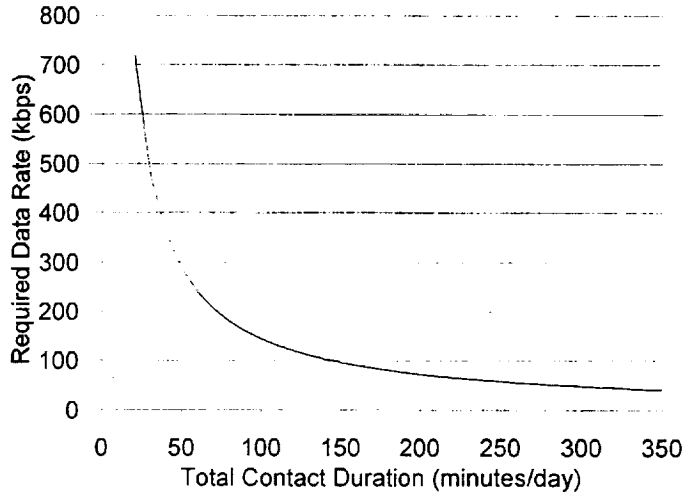

Figure 49 - Required data rate as a function of the total daily contact time.

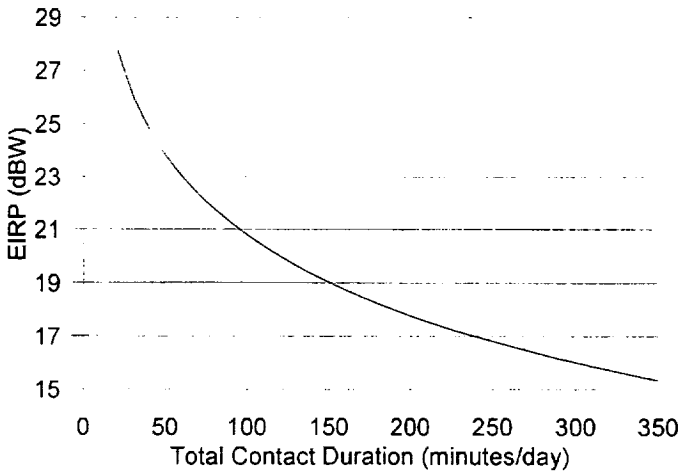

Figure 50 - Required EIRP as a function of the total daily contact time.

Table 19. Typical Contact times, data rates, and EIRP			
TDRS Configuration	**Total Contact Duration (minutes)**	**Data Rate (kbps)**	**EIRP (dBW)**
Single	20	720	27.3
	40	360	24.8
	100	144	20.8
	200	72	17.8
Constellation	60	240	23.0
	120	120	20.0
	240	60	17.0
	300	48	16.0

analysis because the antenna pointing restricted the contact to a shorter portion of the orbit than a full SN access would permit. Using Equation 2 above, the longest path length of 36000 km, and the SMA transmission frequency of 2287.5 MHz, we compute the path loss as

$$L_s = -[32.5 + 20\ log(36000) + 20\ log(2287.5] = -190.81\ dB$$

The minimum EIRP, $EIRP_{min}$, required to support communications at the desired data rate, R_d, is computed using Equation 3 above. Taking the polarization, pointing, and similar losses to be negligible and using the data rate of 16 kbps, the SMA service constant, K, of 221.8, and the space loss computed above yields a $EIRP_{min}$ of 11.05 dBW. The available link margin is the difference between the spacecraft EIRP and $EIRP_{min}$. In this case, the margin is 16.78 dB. This confirms the expectation that the actual performance would be error free since the margin is in excess of 15 dB. This would imply that the data rate can be increased by at least an order of magnitude to in excess of 160 kbps. If a link margin of 3 dB is allowed, a data rate of 382 kbps would be possible under these conditions with a BER of 10^{-5} maintained. Error-correction coding would allow for even higher performance, depending upon the method chosen.

4.3 DESIGN CONSTRAINTS ON ANTENNA GAIN AND EIRP

In order for the concept of using the SN for communications support to be effective, we assume that sufficient transmission power can be obtained from the communications system in the direction of the SN without steering the antenna. A simple method to accomplish this is to have a fairly non-directional antenna system, i.e., one with a large Half-Power Beam Width. The tradeoff for a large HPBW is a low gain for the system thereby giving a low Effective Isotropic Radiated Power. Here

Table 20. TOPEX EIRP Computation		
Parameter	**Value**	**Units**
Transponder Transmission Power	7.05	dBW
P_Q/P_T Loss	-0.12	dB
Filter Loss	-0.2	dB
SC HGA Path Loss	-5.3	dB
HGA Reflector Gain	26.4	dB
Boresight EIRP	27.83	dBW

we will look at how antenna parameters and transmitter power will influence each other to arrive at the required EIRP. In this, we will look at an axial helical antenna system as the basis for the antenna. Then we will determine the required transmitter power based on the antenna gain.

In this study, we made a baseline assumption that an axial-mode helical antenna was available to supply all of the transmission and reception gain. For typical helical antennas, the HPBW and directivity, D, may be computed by using the relationships [22]

$$HPBW = \frac{52^o \lambda^{3/2}}{C\sqrt{NS}}$$

$$D = 15N\frac{C^2 S}{\lambda^3}$$

where C is the helix circumference, N is the number of turns, S is the spacing of the turns ($S = C\ tan(\alpha)$), and λ is the radiation wavelength. Following [23], C was fixed at 0.92λ, the wavelength corresponding to that of the return service frequency through the SN, and the pitch angle, α, was set to 13° in this analysis. Based on [23], the antenna gain is taken to be the computed antenna directivity value. Table 21 lists available HPBW and gains for helix antennas that might be used with the SN S-Band return frequencies.

The Effective Isotropic Radiate Power available with these configurations is given as

$$EIRP\ (dBW) = Pt + Gt - Margin$$

where P_t is the transmitter power in dBW, G_t is the transmission gain from Table 21 and the *Margin* is 3 dB to allow for the pointing loss encountered at the HPBW off-axis angle (i.e., at the start or stop of the service through TDRS). Figure 51 shows the relationship between available EIRP and the available transmitter power. Also shown are lines of data rates possible at various EIRP levels.

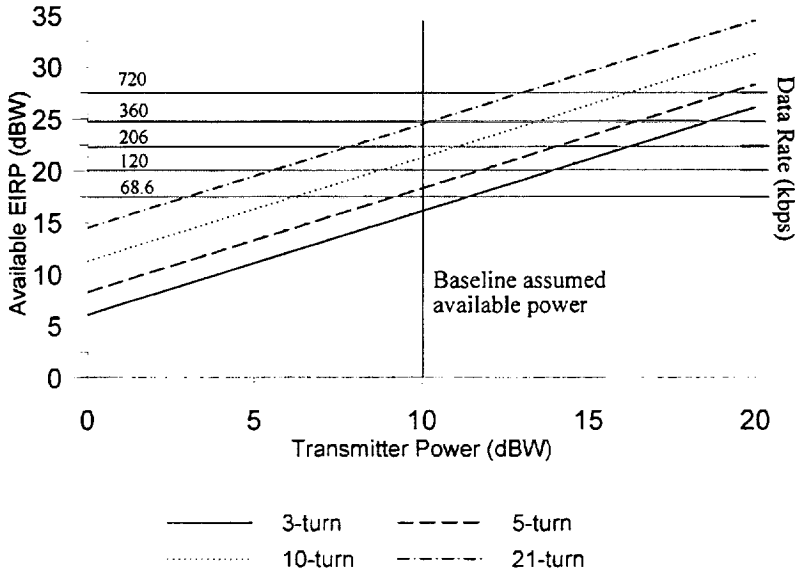

Figure 51 - Available EIRP for axial-mode helical antennas as a function of available transmitter power. Available data rates for the EIRP are also shown.

Table 21. Theoretical Helical Antenna Performance

Number of Turns	Gain (dB)	HPBW
3	9.1	71°
5	11.3	55°
10	14.3	39°
21	17.5	27°

From the above information, we can work backwards and determine the required EIRP and transmitter power to have coverage with the fixed-pointed helical antenna. These results are shown in Table 22. As we can see in this table, there is a trade-off between available contact time and required EIRP at AOS and LOS. While the smaller helical antenna with the wider HPBW and, consequently longer access times, may not be the optimal system. For the 3-turn helical antenna to close the loop and provide the required 10 kbps-equivalent data rate, the system would need to provide an EIRP of 24.7 dBW at AOS/LOS when using the full TDRS constellation. This can be contrasted with the 21-turn helical antenna (incidently, the same size as the antennas in the TDRS SMA array) which needs 28.9

Table 22. Required Performance Using a Helical Antenna System								
No. Turns	Average Contact Duration (min.)		Required Data Rate (kbps)		AOS/LOS EIRP (dBW)		Required Xmit Power (dBW)	
	Single TDRS	Constel-lation	Single TDRS	Constel-lation	Single TDRS	Constel-lation	Single TDRS	Constel-lation
3	12.8	38.6	1125	373	29.5	24.7	20.4	15.6
5	9.78	29.4	1472	490	30.6	25.9	19.3	14.6
10	7.00	21.0	2057	686	32.1	27.3	17.8	13.0
21	4.83	14.5	2981	993	33.7	28.9	16.2	11.4

dBW at the same orbital positions. However, because of the differences in antenna gain between the two configurations, the 3-turn helical system would need a transmitter power of 15.6 dBW while the 21-turn helical system would need a transmitter power of 11.4 dBW. It would therefore seem that to achieve the baseline design goal of a 10-Watt transmitter, the larger helical antenna would be recommended. The exact choice would then be a trade-off between available power, size, and available bandwidth for the entire system. Indications are, however, that the larger antenna sizes should be considered over the smaller antenna sizes.

SECTION 5 - CONCLUSIONS

Based on the experiments run and the analysis performed, we make the following conclusions:

1. The concept of using a fixed antenna system to support a data link through the constellation TDRS satellites in the Space Network offers an alternative to the direct data distribution to a fixed ground station model for data transport. The concept allows for access when the user satellite has an ascending node or descending node of its orbit in the vicinity of a TDRS sub-satellite point.

2. The duration of the contact will be a function of the antenna Half Power Beam Width, orbital inclination angle, and orbital altitude. The HPBW is the primary determinant of the contact duration, the orbital inclination is the second largest contributor to determining the contact duration, and the orbital altitude contributes the least to the contact time. The cases studied here are only for circular orbits. Highly-elliptical orbits were not studied.

3. There will be a trade-off between system antenna parameters, communications transmission power, contact time, and data rate. To achieve a desired data throughput, e.g. 10 kbps equivalent continuous throughput, the required data rate and contact time will be coupled. As the contact time increases, the required data rate to support the throughput will decrease. However, to increase the contact time, one will need to use an antenna with a wider HPBW and lower gain. As the antenna gain decreases, the required transmission power will need to increase to support the transmission. The system designer will need to look at all parameters to decide what is the appropriate data rate, transmission power, antenna gain, and antenna HPBW necessary to support the required service at the desired grade of service.

4. The use of a fixed antenna on inertially-stabilized satellites holds promise as a communications technique. The antenna needs to have a HPBW in excess of 12.4° to maintain contact over the pass. The contact duration at best case will be close to one-half of the orbital period. Wider HPBW antennas will permit coverage on several consecutive orbits and partial coverage on several orbits per day.

5. On inertially-stabilized satellites, the fixed antenna will not give contact on every orbit. Contact with a given TDRS occurs only on those orbits where the antenna is pointed at the TDRS when the satellite is in the vicinity of the TDRS subsatellite point.

SECTION 6 - REFERENCES

[1] S.R. Cvetkovic and G.J. Robertson, "Spacecraft Design Considerations for Small Satellite Remote Sensing," *IEEE Transactions on Aerospace and Electronic Systems*, **AE-29**, April 1993, 391-403.

[2] Small Satellite Working Group, "A Concept for Efficient TDRSS Support to the Small Satellite User Community," Goddard Space Flight Center, TR93152, December 1993.

[3] National Aeronautics and Space Administration, *Space Network (SN) Users' Guide*, revision 7, Goddard Space Flight Center, November 1995.

[4] S. Horan, W. P. Osborne, and T. Minnix, "Improved Small Satellite Access of the Space Network," NMSU-ECE-94-014, December 14, 1994.

[5] S. Horan, "Small Satellite Access of the Space Network," *Proc. 9th Annual AIAA/USU Conference on Small Satellites*, 1995, Supplemental Volume.

[6] S. Horan, "Small Satellite Access of the Space Network," Space Technology and Applications International Forum, AIP Conference Proceedings 361, 1996, p. 501-506.

[7]S. Horan, "Test Report: Low Cost Access and Efficient Use of TDRSS," NMSU-ECE-96-009, July 2, 1996.

[8] S. Horan, "Non-Tracking Antenna Performance for Inertially-Controlled Spacecraft Using TDRSS," submitted to IEEE Trans. Aerospace and Electronic Systems, November 18, 1996.

[9] S. Horan, "Analysis of EUVE Experiment Results," NMSU-ECE-96-016, December 17, 1996.

[10] S. Horan, T. Minnix, and J. Vigil, "Small Satellite Access of the Space Network," submitted to IEEE Trans. Aerospace and Electronic Systems, 1997

[11]S. Horan, "Test Report: Low-Cost Access to TDRS Using TOPEX to Emulate Small Satellite Performance," NMSU-ECE-97-013, September 8, 1997.

[12] Analytical Graphics, Satellite Tool Kit, version 4, 1997.

[13] Warner Miller, NASA Goddard Space Flight Center, 1994, private communication.

[14] NORAD 2-Line Elements, available via anonymous ftp in the directory pub/space at archive.afit.af.mil

[15] V.A. Chobotov, ed., *Orbital Mechanics*, American Institute of Aeronautics and Astronautics,

Reston, VA, 1996, p. 218.

[16]W. L. Stutzman and G. A. Thiele, *Antenna Theory and Design*, 2nd ed., New York: John Wiley & Sons, 1998, p. 321.

[17]T.T. Ha, *Digital Satellite Communications*, 2nd ed., New York: McGraw-Hill, 1990, p. 80.

[18] B. Calanche, Jet Propulsion Laboratory, 1997, private communication.

[19] Stutzman and Thiele, ibid., p. 320

[20] J. Drake, "Experimental EUVE Data Collection and Link Simulation at the STGT," M.S.E.E. Technical Report, New Mexico State University, April 1996.

[21] NASA, *Space Network User's Guide*, Appendix A.

[22] C. A. Balanis, *Antenna Theory Analysis and Design*, 2nd ed., New York: John Wiley & Sons, 1997, p. 510.

[23] Stutzman and Thiele, ibid., p. 235-239.